

Identification of a Signaling Mechanism by Which the Microbiome Regulates Th17 Cell-Mediated Depressive-Like Behaviors in Mice

Eva M. Medina-Rodriguez, Ph.D., Derik Madorma, B.S., Gregory O'Connor, Ph.D., Brittany L. Mason, Ph.D., Dongmei Han, Ph.D., Sapna K. Deo, Ph.D., Mark Oppenheimer, B.S., Charles B. Nemeroff, M.D., Ph.D., Madhukar H. Trivedi, M.D., Sylvia Daunert, Pharm.D., Ph.D., Eléonore Beurel, Ph.D.

Objective: Microbiota dysbiosis has been linked to major depressive disorder, but the mechanisms whereby the microbiota modulates mood remain poorly understood. The authors tested whether specific changes in the microbiome modulate depressive-like behaviors.

Methods: Stools from learned helpless, non-learned helpless, and non-shocked mice were analyzed by V4 16S RNA sequencing to identify gut bacteria associated with learned helplessness and to quantify the level of the quorum-sensing molecule autoinducer-2 (AI-2). T cells were analyzed by flow cytometry, and serum amyloid proteins (SAA) were analyzed by quantitative real-time polymerase chain reaction. Fecal transfer approach and administration of oleic acid and AI-2 were used to determine the effects of the microbiome and quorum-sensing molecules on depressive-like behaviors.

Results: Mice deficient in segmented filamentous bacteria (SFB) were resilient to the induction of depressive-like behavior,

and were resensitized when SFB was reintroduced in the gut. SFB produces the quorum-sensing AI-2 and promotes the production of SAA1 and SAA2 by the host, which increases T helper 17 (Th17) cell production. Th17 cells were required to promote depressive-like behaviors by AI-2, as AI-2 administration did not promote susceptibility to depressive-like behaviors or SAA1 and SAA2 production in Th17-deficient mice after stress. Oleic acid, an AI-2 inhibitor, exhibited antidepressant properties, reducing depressive-like behavior, intestinal SAA1 and SAA2 production, and hippocampal Th17 cell accumulation. Stool samples from 10 people with current depressive symptoms and 10 matched healthy control subjects were analyzed as well. Patients with current major depressive disorder exhibited increased fecal interleukin 17A, SAA, and SFB levels.

Conclusions: The study results reveal a novel mechanism by which bacteria alter mood.

Am J Psychiatry 2020; 177:974–990; doi: 10.1176/appi.ajp.2020.19090960

Major depressive disorder is a debilitating disease with a lifetime incidence of ~20% (1). Current treatments often lack efficacy and take several weeks to be effective. Recent evidence has pointed toward a role of the gut microbiome composition in exacerbating psychiatric disorders, including major depression (2). The microbiota within the gut influences gut-brain communication and behavior (for a review, see reference 3). The bidirectional communication between the gut and the brain is thought to involve neural, hormonal, and immunological routes, including the sympathetic and parasympathetic arms of the autonomic nervous system and the enteric nervous system. Dysregulation of this communication often leads to pathophysiological effects (4).

There are well-documented effects of changes in the composition of the microbiota on behavior and cognition (5). Microbiota changes have often been studied by using germ-free

animals, bacterial infection, and probiotic treatments. For example, the absence of the microbiome, such as in germ-free mice, has been associated with increased susceptibility to stress, and this can be reversed by administration of *Bifidobacterium infantis* harvested from the feces of the specific pathogen-free control animals (6). Moreover, the earlier the colonization occurs, the better the outcome. De Palma et al. (7) showed that germ-free mice were less immobile in the tail suspension test of depression-like behavior than conventional mice, suggesting an antidepressant action of depleting the microbiota in mice. Conversely, transfer of a human fecal microbiota from depressed patients to germ-free mice conferred a depressive-like behavior to the mice compared with mice receiving microbiota from healthy patients, showing that dysbiosis of the gut microbiome can promote depressive-like behaviors in mice (8).

See related feature: **Editorial** by Ms. Cruz-Pereira and Dr. Cryan (p. 895)

The microbiota can be influenced by many factors, including diet, exercise, and infection, and stress is a major factor that is relevant for depression (9–11). Substantial evidence demonstrates that activation of the hypothalamic-pituitary-adrenal (HPA) axis influences the composition of the gut microbiota. Maternal separation in rhesus monkeys, which increases HPA axis activity, was found to result in a reduction of fecal bacteria, especially *Lactobacilli* (12, 13), and early-life stress in rats or chronic restraint stress in adult rodents also changed the composition of the gut microbiota (14), in conjunction with increasing proinflammatory cytokines and chemokines (15). Chronic restraint stress also increases the permeability of the gut, leading to the disruption of the gut barrier (leaky gut) and the release of lipopolysaccharides into the circulation (16, 17). This can be reversed, however, by probiotic agents (13, 17, 18). Patients with major depression exhibit significant changes in the relative abundance of Firmicutes, Actinobacteria, and Bacteroidetes compared with healthy individuals (8), and administration of the probiotic *Lactobacillus farciminis* has been shown to prevent the gut leakage and the activation of the HPA axis (19, 20), confirming the critical role of the microbiota in the gut-brain dialogue and the potential beneficial role of probiotic treatments in major depression (21). A variety of mechanisms of action of probiotics have been proposed, such as 1) down-regulating the HPA axis, which is often overactive in patients with major depression (22); 2) promoting biosynthesis of GABA, levels of which are reduced in patients with major depression (23); and 3) increasing the production of tryptophan and therefore the serotonin level (24). Altogether, gut dysbiosis is often evident in patients with major depression and in mice exhibiting depressive-like behaviors (8, 25–29; for a review, see reference 30), suggesting a dysregulation of the brain-gut axis in depression. However, molecular mediators of the effects of the microbiota in depressive-like behaviors remain to be identified.

Besides regulating brain responses to stress and behavior, the microbiota also dramatically regulates the immune system (31, 32). Recent studies have shown the importance of host-specific species such as the segmented filamentous bacteria (SFB), also called “*Candidatus* Arthromitus.” SFB is a nonculturable spore-forming Gram-positive bacterium that is most closely related to the genus *Clostridium* and colonizes the intestines of numerous species, including humans (33). Mouse gut colonization by SFB is required for the maturation of the innate and the adaptive immune systems (34, 35). This is relevant for depression because critical roles of the innate and adaptive immune systems have been shown to regulate the susceptibility to depressive-like behaviors in mice (36–38). T cells express the surface marker, CD4, that is used to identify them as CD4⁺, and one type of T cell, the T helper (Th) 17 cell that produces the signature cytokine interleukin 17A (IL-17A), is known to be toxic to the CNS in autoimmune diseases (39). We recently found that Th17 cells were sufficient to increase susceptibility to depressive-like behaviors in mice (40). Th17 cells are only present in the lamina propria of the small intestine in

healthy mice (34), and they are pathogenic when they infiltrate the CNS, such as in multiple sclerosis (41). Thus, it is particularly relevant that Th17 cells are highly up-regulated by SFB (34, 42). Without SFB, Th17 cells are absent in the mouse small intestinal lamina propria, where they are usually abundant in normal healthy rodents in the presence of commensal microbiota (34). Introduction of SFB in mice that are deficient in Th17 cells induces the production of Th17 cells (34).

Here, we tested whether changes in the microbiome modulate depressive-like behaviors, and found that mice deficient in SFB are resilient to the induction of depressive-like behaviors, and that introduction of SFB in SFB-deficient mice reestablished susceptibility to depressive-like behaviors. Bacteria communicate, detect, and respond to cell population density by releasing quorum-sensing molecules (43). SFB produce the quorum-sensing molecule autoinducer-2 (AI-2), a furanosyl borate diester or tetrahydroxy furan (IUPAC name: (3aS,6S,6aR)-2,2,6,6a-tetrahydroxy-3a-methyltetrahydrofuro[3,2-d][1,3,2]dioxaborolan-2-uide), and administration of AI-2 induced a host response, comprising serum amyloid protein-1 (SAA1) and SAA2 production, and promoted depressive-like behaviors in a Th17 cell-dependent manner. These experiments identified an SFB/AI-2/Th17 cell circuit as contributing to the increased susceptibility to depressive-like behaviors, uncovering the previously unknown role of bacterial AI-2 in modulating behavior.

METHODS

Mice

We used 6- to 12-week-old wild-type C57BL/6, *Rorc*(γ T)^{+/GFP}, *Rag2*^{−/−}, or 7B8 (Tg(Tcra,Tcrb)2Litt/J, strain 027230), IL17A-IRES-GFP-KI (strain 018472) male mice. C57BL/6 mice were either bred in the University of Miami animal facility or purchased from Taconic Biosciences (TAC) or Jackson Laboratory (JAX). The *Rorc*(γ T)^{+/GFP} mice (strain 007572 [44]) were obtained by crossing *Rorc*(γ T)^{+/GFP} × *Rorc*(γ T)^{+/GFP} to produce 50% *Rorc*(γ T)^{+/GFP}, 25% wild-type, and 25% *Rorc*(γ T)^{GFP/GFP} mice, and littermates were used. *Rorc*(γ T)^{GFP/GFP} mice were not used because their locomotor activity is altered, compromising the interpretation of the behavioral testing. Mice were housed in light- and temperature-controlled rooms and treated in accordance with National Institutes of Health and the University of Miami Institutional Animal Care and Use Committee regulations.

Treatments

Mice were injected intraperitoneally with 5 nmol of AI-2 (Omm Scientific, Dallas; vehicle is saline), short-chain acyl homoserine lactone (sc-AHL) (chain of 6 carbons) (Sigma-Aldrich, St. Louis; vehicle is saline), or oleic acid (Sigma-Aldrich, St. Louis; vehicle is saline with 5% DMSO, 5% Tween80), or 5 μ g of mouse recombinant SAA2 (MyBioSource, San Diego; vehicle is saline), as indicated within each experiment.

Behavioral Assessments

Learned helplessness. Learned helplessness was measured using a standard learned helplessness paradigm or a modified reduced inescapable foot shock protocol, as described previously (40, 45). The reduced paradigm was used so that wild-type C57BL/6 mice did not develop learned helplessness, allowing measurements of increased susceptibility to learned helplessness. Briefly, mice were placed in one side of a Gemini avoidance system shuttle box (Med Associates, St. Albans, Vt.) with the gate between chambers closed. For standard learned helplessness, 180 inescapable foot shocks were delivered at an amplitude of 0.3 mA, a duration of 6–10 seconds per shock, and a randomized intershock interval of 5–45 seconds (40). In a modified inescapable shock protocol, referred to as the reduced learned helplessness protocol, mice were given 180 foot shocks with amplitude of 0.3 mA and a 2- to 6-second shock duration, and a randomized intershock interval of 5–45 seconds (45). Twenty-four hours after the inescapable foot shocks, mice were returned to the shuttle box and the number of escapes from 30 escape trials was recorded. Each trial uses a 0.3 mA foot shock for a maximum duration of 24 seconds. The door of the chamber opens at the beginning of the foot shock administration to allow the mouse to escape. Trials in which the mouse did not escape within the 24-second time limit were counted as escape failures. Mice with >15 escape failures were defined as learned helpless. For the long-term paradigm, mice subjected to the standard learned helplessness were retested with escapable foot shocks once a week over a maximum of 4 weeks (46).

Tail suspension test. For the tail suspension test, mice were suspended by the tail in an automated tail suspension test cubicle (33×31.75×33 cm; Med Associates) for a period of 6 minutes, and the immobile time was analyzed for the last 4 minutes, using Med Associates software.

Open field. Locomotor activity in an open field apparatus was measured as previously described (40). Briefly, mice were placed in a Plexiglas open field (San Diego Instruments, San Diego) outfitted with photobeam detectors under soft overhead lighting, and activity was monitored over 30 minutes using activity monitoring software (San Diego Instruments).

Social interactions. For the three-chambered social interaction test (40), the apparatus was a transparent rectangular Plexiglas box divided by Plexiglas walls into three equal-sized connected chambers with an empty wire enclosure in the two end chambers. The day before testing, the test mice were habituated individually by being allowed to freely explore the entire apparatus for 20 minutes and, separately, an unfamiliar, conspecific, same-sex stimulus mouse was habituated for 20 minutes in the wire enclosure in one of the chambers. On the day of the test, the test mouse was placed in the center of the middle chamber and allowed to freely explore the entire apparatus for 5 minutes. The test mouse was allowed to explore the entire apparatus for 10 minutes with the unfamiliar mouse placed in

one of the chambers on the side of the box. Each session was videotaped and quantified for time spent in each chamber and for number of nose contacts with the stimulus mouse.

SFB Colonization

The colonization by SFB was achieved by either ad libitum cohousing 5–6 week old age-matched male mice in sterilized cages for 2 weeks at a ratio of 2:3 JAX to TAC mice, as previously described (47), or by gavage of 100 μ L of fecal homogenates of SFB monocolonized mice in water (34). SFB colonization after 2 weeks was confirmed by quantitative polymerase chain reaction (qPCR). Control JAX mice were gavaged with homogenates of their own feces in water.

SFB qPCR

Genomic DNA was purified from stools using the Quick-DNA Fecal/Soil Microbe Miniprep (Zymo Research, Irvine, Calif.) according to the manufacturer's instructions. SFB gene expression (SFB primers: 5'-ACGCTACATCGTCTTATCTTCCCGC-3' and 5'-TCCCCAAGACCAAGTTCACG-3') was assessed by SYBR qPCR in a qTOWER instrument from Analytik Jena and the results were quantified by the $2^{-\Delta\Delta C_t}$ method. Values were normalized to *Eubacteria* (EUB primers: 5'-ACTCC TACGGGAGGCAGCAGT-3' and 5'-ATTACCGCGGCTGCTG GC-3') for each sample.

Quorum Sensing Molecule Measurement

Fecal homogenates were incubated with bacteria expressing the plasmids pSB406 (sc-AHL), pSB1075 (long-chain acyl homoserine lactone, lc-AHL), or MM32 (AI-2). The same amount of feces weight was used. Briefly, for measuring AHLs, *E. coli* DH5a bacteria expressing pSB1075 or pSB406 were grown in lysogeny broth (LB) containing 100 μ g/mL ampicillin at 37°C with orbital shaking, and for measuring AI-2, *Vibrio Harveyi* bacteria were grown overnight in M9 medium containing 30 μ g/mL kanamycin, at 30°C with orbital shaking (250 rpm). Stools were homogenized in water and diluted 1:1600 (AHL) or 1:750 (AI-2) and incubated for 2 hours (AHLs) or 2.5 hours (AI-2) with these bacteria at 37°C (AHL) or 30°C (AI-2), with orbital shaking at 175 rpm. Bioluminescence was assessed using a standard curve with commercial AHL or AI-2 (Sigma-Aldrich or Omm Scientific). The induced luminescence intensity was measured using a microplate reader (BMG Labtech Polar Star Optima microplate luminometer, Ortenberg, Germany). All luminescent intensities were reported as the average of a minimum of three replicates that are blank subtracted and are expressed in relative light units.

Microbiome Sequencing

V4 16S RNA sequencing was performed by Second Genome (South San Francisco, Calif.). Briefly, nucleic acid isolation was achieved with the MoBio PowerMag Microbiome kit (Mo Bio Laboratories, Carlsbad, Calif.) according to the manufacturer's instructions and optimized for high-throughput processing. All samples were quantified via the Qubit Quant-iT

dsDNA High Sensitivity Kit (Invitrogen, Life Technologies, Grand Island, N.Y.).

For the library preparation, each sample was PCR amplified with two differently bar-coded V4 fusion primers and concentrated using a solid-phase reversible immobilization method for the purification of PCR products and quantified by qPCR. Samples were paired-end sequenced using a MiSeq instrument (Illumina, San Diego) according to the manufacturer's instructions. Reads were merged using USEARCH, and the resulting sequences were compared with an in-house strains database using USEARCH (usearch_global). All sequences hitting a unique strain with an identity $\geq 99\%$ were assigned a strain operation taxonomic unit (OTU). To ensure specificity of the strain hits, a difference of $\geq 0.25\%$ between the identity of the best hit and the second best hit was required. For each strain OTU, one of the matching reads was selected as representative and all sequences were mapped by USEARCH (usearch_global) against the strain OTU representatives to calculate strain abundances. The remaining non-strain sequences were quality filtered and dereplicated with USEARCH. Resulting unique sequences were then clustered at 97% by UPARSE, and a representative consensus sequence per de novo OTU was determined. Representative OTU sequences were assigned taxonomic classification via the mothur Bayesian classifier, trained against the Greengenes reference database of 16S rRNA gene sequences clustered at 99%. All profiles are intercompared in a pairwise fashion to determine a dissimilarity score and stored in a distance dissimilarity matrix, using the Bray-Curtis dissimilarity. The binary dissimilarity values were calculated with the Jaccard index and represented using dendrograms and analyzed using permutational analysis of variance. Univariate differential abundance of OTUs was tested using a negative binomial noise model for the overdispersion and Poisson process intrinsic to these data, as implemented in the DESeq2 package (48, 49). DESeq q-values were corrected using the Benjamini-Hochberg procedure. All the data were deposited in the Sequence Read Archive (SRA), BioProject PRJNA498103.

Antibiotic Treatment

Specific-pathogen-free (SPF) mice were gavaged with a solution of neomycin (100 mg/kg), metronidazole (100 mg/kg), and vancomycin (50 mg/kg) twice daily for 7 days before starting the injections of AI-2, and antibiotic treatments were continued until the behavioral assessments were finished to avoid bacterial recolonization, using dosages typically greater than those used for clinical therapeutic treatment. Ampicillin (1 mg/mL) was also provided ad libitum in drinking water. These conditions produced germ-free-like phenotype (50). Bacterial depletion was evaluated by *Eubacteria* 16S qPCR. The level of *Eubacteria* was 99.9% depleted (see Figure S1F in the online supplement), confirming depletion of the microbiota with the antibiotic regimen.

Adoptive Transfer

CD4⁺ cells were isolated as described previously (33). Approximately 1×10^6 undifferentiated CD4 cells were injected intravenously in 200 μ L phosphate-buffered saline (PBS) by tail vein 48 hours before behavioral testing or as indicated in Figure S2H–I in the online supplement. Depending on the number of mice to be injected, cells transferred were pooled from 1–2 donors.

SAA, IL-22 Quantitative Real-Time PCR (qRT-PCR)

The most distal part of the small intestine was dissected and rinsed and Peyer's patches were removed. RNA was extracted with TRIzol Reagent (Life Technologies) and cDNA was synthesized with ImProm-II Reverse Transcriptase and random primers (Promega, Madison, Wisc.). SAA1, SAA2, SAA3 (34), and IL-22 expression was measured by SYBR green RT-qPCR in a qTOWER instrument from Analytik Jena and the results were quantified by the $2^{-\Delta\Delta C_t}$ method. The primers used were SAA1: 5'-CATTTGTTCCAGGAGCTTCC-3' and 5'-GTTTTTCCAGTTAGCTTCCTTCATGT-3'; SAA2: 5'-TGTGTATCCCACAAG GTTTCAGA-3' and 5'-TTATTAC CCTCTCCTCTCAAGCA-3'; SAA3: 5'-CGCAGCACGAGCAG GAT-3' and 5'-CCAGGATCAAGATGCAAAGAATG-3'; IL-22: 5'-AGAACGTCTTCCAGGGTGAA-3' and 5'-TCCGAGGAGT CAGTGCTAAA-3'. Values were normalized to glyceraldehyde-3-phosphate dehydrogenase (GAPDH) (primers: 5'-AGGTCGG TGTGAACGGATTG-3' and 5'-TG TAGACCATGTAGT TGAGGTCA-3').

Flow Cytometry

Immediately after learned helplessness, mice were anesthetized, spleens were recovered, and mice were transcardially perfused with PBS as previously described (40, 45). Briefly, the hippocampi were dissected, excluding meninges and choroid plexus, passed through a 70- μ m cell strainer (BD Biosciences, San Jose, Calif.), and the cell suspension was mixed (vol/vol) to obtain a 30% Percoll/R1 medium (RPMI 1640 medium [Corning] supplemented with 1% fetal bovine serum [Gibco], 100 IU/mL penicillin [Gibco], 100 μ g/mL streptomycin [Gibco], 1 \times nonessential amino acids [Gibco], 1 μ M sodium pyruvate [Gibco], 2.5 μ M β -mercaptoethanol [Sigma-Aldrich] and 2 mM L-glutamine [Gibco]). The cellular suspension was overlaid on 70% Percoll/R1 medium in a centrifuge tube and centrifuged at 2000 rpm for 20 minutes without using the brake. The cells at the interface of the 30%/70% Percoll gradient were recovered, washed once, resuspended in R10 media and stimulated for 4 hours with phorbol myristate acetate (50 ng/mL; Sigma-Aldrich) and ionomycin (750 ng/mL; Sigma-Aldrich) in the presence of Protein Transport Inhibitor Cocktail (eBioscience) at the recommended concentrations. Standard intracellular cytokine staining was carried out as described elsewhere (33) using the Staining Intracellular Antigens for Flow Cytometry Protocol (eBioscience). Cells were first stained extracellularly with BV480-conjugated anti-CD4 (BD Biosciences), then fixed and permeabilized with permeabilization solution (eBioscience), and finally

intracellularly stained with BV650-conjugated anti-IFN- γ (BD Biosciences), phycoerythrin-conjugated anti-IL-17A (eBioscience) and BV421-conjugated anti-FoxP3 (BD Bioscience). Samples were acquired on a FACS CELESTA (BD Biosciences) and data were analyzed with the FlowJo software program (Tree Star, Inc.).

Immunohistochemistry

Immediately after learned helplessness escapable-shock testing, mice were anesthetized, spleens were recovered, and mice were transcardially perfused with PBS as described above. Brains were fixed with 4% PFA, postfixed, cryo-protected in sucrose, and then snap-frozen in optimal cutting temperature reagent and stored at -80°C . Twenty-micrometer sections were stained for GFP (anti-GFP Chicken, catalog number 1020, Aves Labs) and Dapi and imaged on an EVOS FL fluorescent microscope (Life Technologies).

Gut Permeability

To measure gut permeability (modified from reference 51), mice were gavaged with FITC-Dextran (Sigma-Aldrich; 600 mg/kg in 100 μL of PBS) 4 hours before sacrifice. Mice were anesthetized and blood was collected at the time of sacrifice via hepatic vein and spun down to collect serum. Fluorescence was measured at 490 nm (excitation) and 530 nm (emission) in serum samples diluted 1:1 with PBS.

Cytokine Measurements

Serum cytokines were measured in 12.5 μL of serum using multiplexing measuring 26 cytokines and chemokines according to the manufacturer's instructions (mouse cytokine/chemokine, 26 Plex, catalog number EPX260-26088-901, eBioscience) on a MAGPIX instrument (Luminex).

Human Samples

Stool samples from 10 participants with current depressive symptoms, defined as a score ≥ 13 on the Quick Inventory of Depressive Symptomatology (QIDS), and 10 matched healthy control subjects were analyzed (for demographic information, see in Table S1 in the online supplement) from an ongoing longitudinal study at the University of Texas Southwestern Medical Center. Samples were collected by participants at home, frozen upon collection, transported frozen back to the center, and then stored at -80°C until analysis.

Eighty percent of the depressed samples had a primary diagnosis of major depressive disorder, and the remaining psychiatric samples had bipolar disorder diagnoses. Psychiatric state at the time of sample collection, assessed by the Longitudinal Interval Follow-Up Evaluation (LIFE) (52), confirmed the incidence of a full depressive episode or an episode in partial remission for all. In addition, the majority of the psychiatric samples had marked or fully expressed generalized anxiety disorder or other anxiety disorders, and two participants experienced mania or hypomania within 2 weeks of sample collection. One participant's LIFE data were not available. The healthy control samples had no diagnosed psychiatric disorders.

The study was approved by the University of Texas Southwestern Institutional Review Board. Informed consent was obtained from all participants.

Human IL-17A and SAA Measurement

Stool samples were homogenized (100 mg/mL) in PBS supplemented with 1 $\mu\text{g/mL}$ leupeptin, pepstatin, and 1 mM phenylmethylsulfonyl fluoride, sonicated and centrifuged for 15 minutes at 10,000 g at 4°C . IL-17A and SAA were measured in 25 μL of stool homogenates using human IL-17A Simplex and SAA Simplex Procarta multiplex assays (catalog numbers EXP01A-12136-901, EXP01A-12017-901, Thermo Fisher Scientific) on a MAGPIX instrument (Luminex). Samples were run on one plate, blind to treatment. Assays were checked for quality control to fit the standard curves. Two samples (one from a healthy control subject, one from a participant with major depression who had a primary bipolar diagnosis) were not used for IL-17A and SAA measures because of the nature of the stools (diarrhea), for which 50 mg of actual stool could not be sampled to get protein concentrations consistent with the other samples. This issue did not affect quorum-sensing molecule measurements because they are chemicals measured on the basis of tissue weight rather than protein concentration. Points were excluded if the values deviated more than three standard deviations from the mean and were considered statistically outlier values. For all analyses, any samples that were under the detection limit were excluded. The data were analyzed in SPSS, version 24 (IBM, Armonk, N.Y.).

Human SFB and QSM Measurement

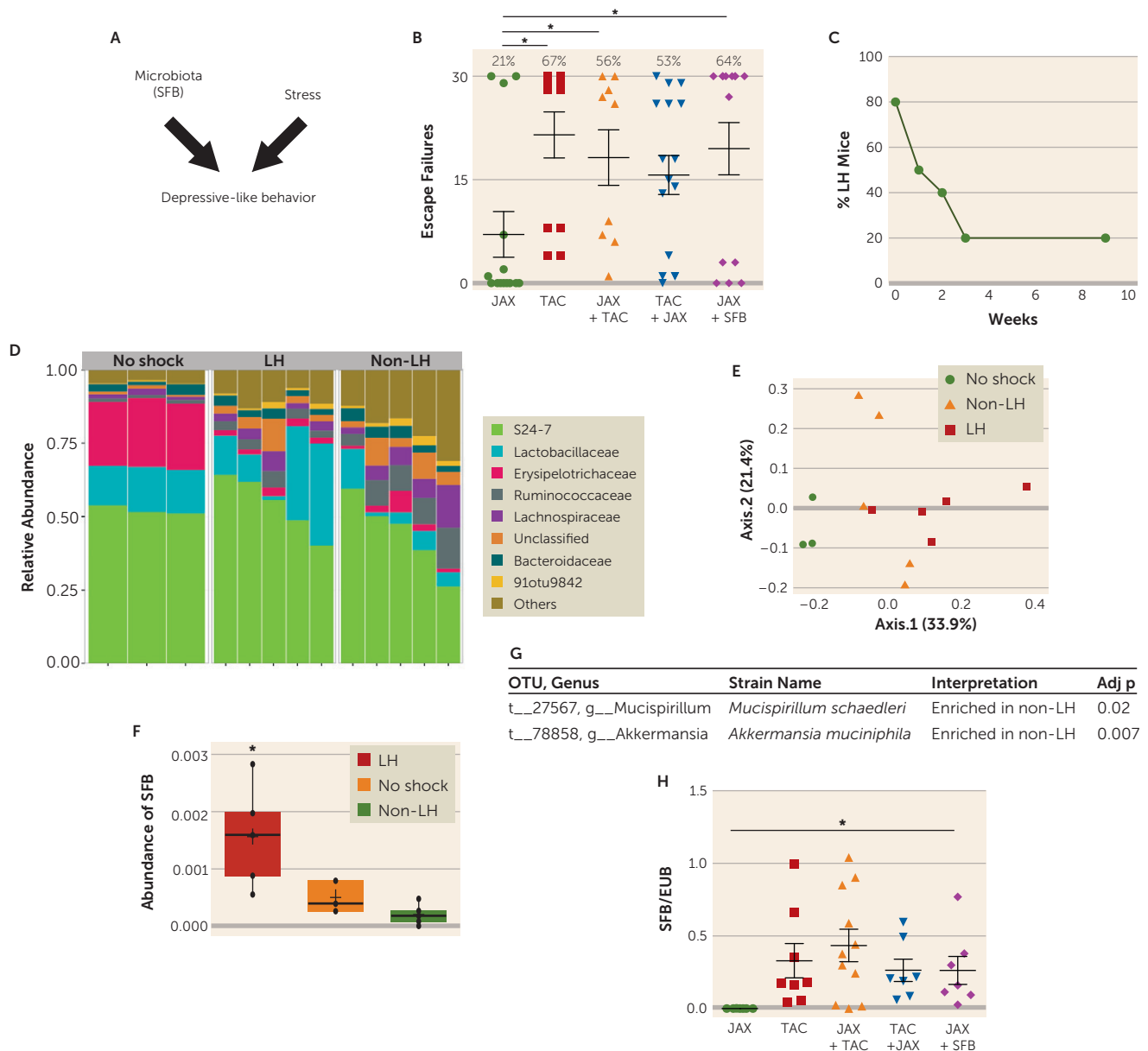
For SFB measurements, genomic DNA was extracted using the Quick-DNA Fecal/Soil Microbe Miniprep (Zymo Research) according to the manufacturer's instructions, and amplified by PCR as described above. Points were excluded if the values deviated more than three standard deviations from the mean and were considered outlier values. For the QSM measurements, similar approaches to those for mouse were used, as described above.

Statistical Analysis

Data are represented as means and standard errors of the mean. Statistical significance was analyzed with a one-way analysis of variance for multiple comparisons with the Bonferroni post hoc test or with Student's *t* test or the Mann-Whitney *U* test using the Prism program when appropriate. Pearson correlations were computed in SPSS, version 24. The threshold for statistical significance was set at a *p* value of 0.05. All statistical tests were two-sided.

RESULTS

To determine whether the composition of the gut microbiome can affect sensitivity to the foot shock-induced learned helplessness model of depression (Figure 1A), we tested the sensitivity to the induction of learned helplessness of mice

FIGURE 1. Higher levels of segmented filamentous bacteria (SFB) in learned helpless mice^a

^a Panel A is a schematic diagram of the experiment. In panel B, JAX and TAC mice were housed with or without mice from the other source for 2 weeks, or JAX mice were gavaged with SFB or their own feces as control, and then mice were subjected to the learned helplessness paradigm. Escape failures were recorded, and means (with standard error of the mean) of the escape failures are displayed, and the percentage of mice exhibiting learned helplessness (failing to escape in >15 of the 30 trials) is shown above each group. Each symbol represents an individual mouse. Since both displayed resistance to learned helplessness, results were combined for untreated JAX mice (1/7 developed learned helplessness; average, 5 escape failures) and JAX mice gavaged with their own feces (2/7 developed learned helplessness; average, 8 escape failures). (N=9–16, one-way analysis of variance [ANOVA], $F=2.523$, $df=4, 57$; $*p<0.05$ Bonferroni post hoc test.) In panel C, TAC mice were subjected to learned helplessness and retested with only escapable shocks after 1, 2, 3, and 9 weeks, and the percentage of learned helpless (LH) mice was calculated after each test (N=15). In panels D–G, stools were collected from mice tested in panel C after 4 weeks, and V4 16S RNA gene sequencing was carried out by Second Genome. Panel D illustrates the proportional abundance in LH mice (N=5), non-LH mice (failed to escape in <15 of 30 trials every week for 4 weeks; N=5), or mice receiving no shock (N=3); the plot shows the most abundant taxa at the family level. (The 91otu9348 16S sequence included in panel D existed in the public domain but was not closely related to any known, named bacterial sequences at the time of sequencing.) Panel E is a weighted ordination plot showing dimensional reduction of the Bray-Curtis distance between microbiome samples, using the principal coordinate analysis method. OTU=operation taxonomic unit. Panels F and G summarize the main strain differences. Panel F shows that the relative abundance of SFB compared with other OTUs in the same community is increased in learned helpless mice. Panel G shows that the relative abundance of *Mucispirillum schaedleri* and *Akkermansia muciniphila* compared with other OTUs in the same community is decreased in learned helpless mice. (Kruskal-Wallis rank sum test with Bonferroni correction, $*p=0.007$; N=5 mice per group compared with non-LH mice.) In panel H, SFB levels, presented as the ratio of SFB to eubacteria (EUB), were measured prior to learned helplessness induction in each group shown in panel B. (N=7–11; one-way ANOVA, $F=2.612$, $df=4, 39$, $*p<0.05$ Bonferroni post hoc test.)

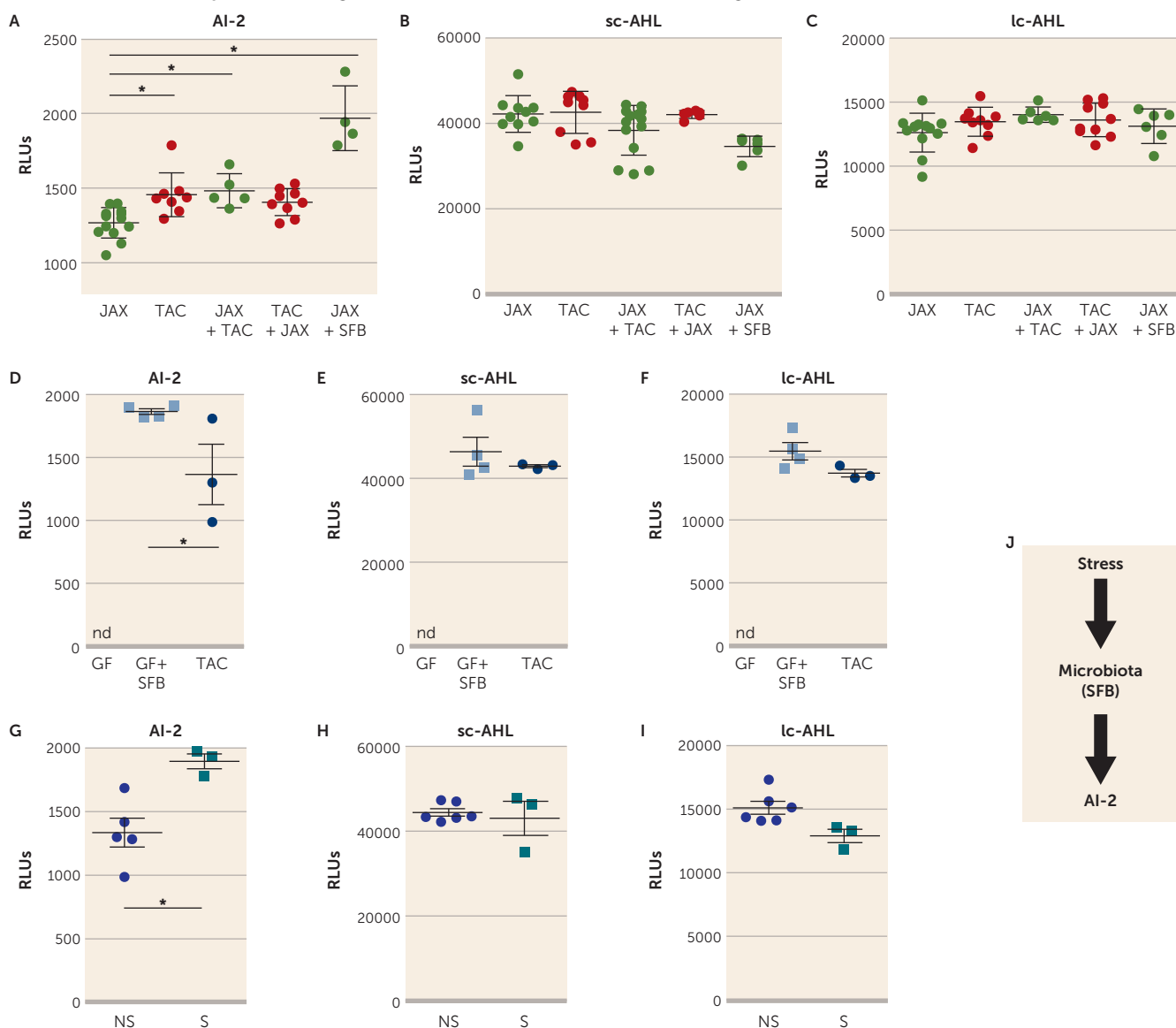
obtained from the Jackson Laboratory (JAX) or Taconic Farms (TAC), which have different microbiomes (34). We found that only 21% of JAX mice, but 67% of TAC mice, exhibited learned helplessness (Figure 1B), showing that TAC mice were significantly more susceptible to the induction of learned helplessness than JAX mice. We next tested whether cohousing JAX and TAC mice, which allows sharing of microbiota between cohoused mice, changed their susceptibility to learned helplessness. After cohabitation for 15 days, 56% of JAX mice and 53% of TAC mice exhibited learned helplessness (Figure 1B). This suggests that JAX mice that acquire the microbiota of TAC mice (34) display increased susceptibility to learned helplessness compared with naive JAX mice, averaging 18 failures out of the 30 escape trials, compared with eight failures without cohousing, whereas the susceptibility of TAC mice remained essentially unchanged by cohabitation. This raises the possibility that bacteria in the TAC mice microbiota increase sensitivity to learned helplessness, and/or the microbiota of JAX mice provides resilience to learned helplessness.

To identify bacteria that may modulate learned helplessness, TAC mice were retested every week to identify mice that maintained learned helplessness for a long period of time (Figure 1C). For this, we used the paradigm of learned helplessness we described previously (40), in which ~20% of the mice keep exhibiting learned helplessness after 3–9 weeks of retesting (Figure 1C). This differs from the behavior of most mice, as ~80% of mice spontaneously recover from learned helplessness within 3 weeks, demonstrating a difference in 20% of mice that blocks recovery from this depression-like behavior. We performed V4 16S rRNA sequencing to identify the bacteria that are different in mouse stools immediately after exposure to escapable foot shocks (to differentiate mice that are either susceptible or resilient to learned helplessness) and in mice that maintain learned helplessness for 4 weeks (Figure 1D–E). We ensured that a complete microbiome profile was captured because the number of sequences per sample ranged from 111,769 to 162,600 filtered reads. We found no change in the alpha diversity metric, and the average number of OTUs per sample and per group ranged from 342 to 368, with an average Shannon diversity index per group range of 2.77–3.47. There were no differences among groups at the level of phyla. However, at the family level, Erysipelotrichaceae was lower in mice 4 weeks after receiving inescapable foot shocks whether they exhibited (2.26%) or did not exhibit learned helplessness (2.89%) than in mice that did not receive foot shocks (mean 22.7%) (Figure 1D). Thus, the stress of the learned helplessness paradigm was sufficient to cause this large difference in the microbiota independently of the behavioral outcome. There were six significantly different OTUs detected, out of 497 examined in mice displaying learned helplessness for 4 weeks compared with mice that underwent the learned helplessness paradigm but never displayed learned helplessness. *Akkermansia muciniphila* (one OTU) and *Mucispirillum schaedleri* (two OTUs) were enriched in non-learned helpless samples (Figure 1G),

whereas SFB (one OTU) and two unclassified OTUs from the order Clostridiales were enriched in mice that displayed learned helplessness for 4 weeks (Figure 1F). Thus, the microbiome is significantly different in mice that are resilient to learned helplessness and mice that are susceptible to and maintain prolonged learned helplessness.

The elevated SFB level in mice that exhibited prolonged learned helplessness compared with resilient mice raised the possibility that SFB may promote learned helplessness. Interestingly, JAX mice, which are resistant to learned helplessness, are known to be deficient in SFB (Figure 1H) (34), and we found that JAX mice cohoused with TAC mice express fecal SFB similar to TAC mice (Figure 1H) as well as exhibiting similar susceptibility to learned helplessness (Figure 1B). We tested whether SFB is sufficient to increase susceptibility to learned helplessness by gavaging JAX mice with SFB-monocolonized feces and subjecting them to learned helplessness. After the introduction of SFB, 64% of JAX mice exhibited learned helplessness (compared with 21% in control JAX mice), within an average of 20 failures out of 30 trials (Figure 1B). These results indicate that the presence of SFB in the microbiota promotes susceptibility to learned helplessness, but they do not rule out the likelihood that other microbiota components also are modulatory, such as *Akkermansia muciniphila* and *Mucispirillum schaedleri*.

To identify a mechanism by which bacteria in the microbiome may influence depression-like behaviors, we examined quorum-sensing molecules (QSMs). QSMs are uniquely secreted by bacteria in response to changes in population density to coordinate several bacterial behaviors, including biofilm formation, swarming, and virulence gene expression, as well as to modulate antibiotic resistance (53, 54). We hypothesized that QSMs, which would reflect overall changes in bacteria species in the gut, contribute to microbiome-modulated susceptibility to learned helplessness. We analyzed three major QSMs in the feces of the JAX, TAC, and cohoused mice: autoinducer-2 (AI-2), short-chain AHL (sc-AHL), and long-chain AHL (lc-AHL). The fecal AI-2 level was significantly increased in TAC mice or JAX mice cohoused with TAC mice compared with JAX mice alone (Figure 2A). The abundance of sc-AHL and lc-AHL was similar among all groups (Figure 2B–C). Reintroduction of SFB in JAX mice was sufficient to significantly increase AI-2 levels but not sc-AHL or lc-AHL (Figure 2A–C). We confirmed that AI-2 can be produced by SFB, as the fecal AI-2 level was increased in germ-free mice monocolonized with SFB compared with TAC mice (Figure 2D), whereas sc-AHL or lc-AHL levels were similar in these two groups (Figure 2E–F), suggesting that AI-2, sc-AHL, and lc-AHL were all produced by SFB, but that AI-2 might be preferentially expressed in SFB monocolonized mice (Figure 2D). Germ-free mice do not produce AI-2, sc-AHL, or lc-AHL (Figure 2D–F). We also determined whether foot shock stress used for inducing learned helplessness induced AI-2 levels. TAC mice subjected to the 48-hour paradigm of learned helplessness had a higher level of AI-2 than TAC mice that did not receive foot shocks

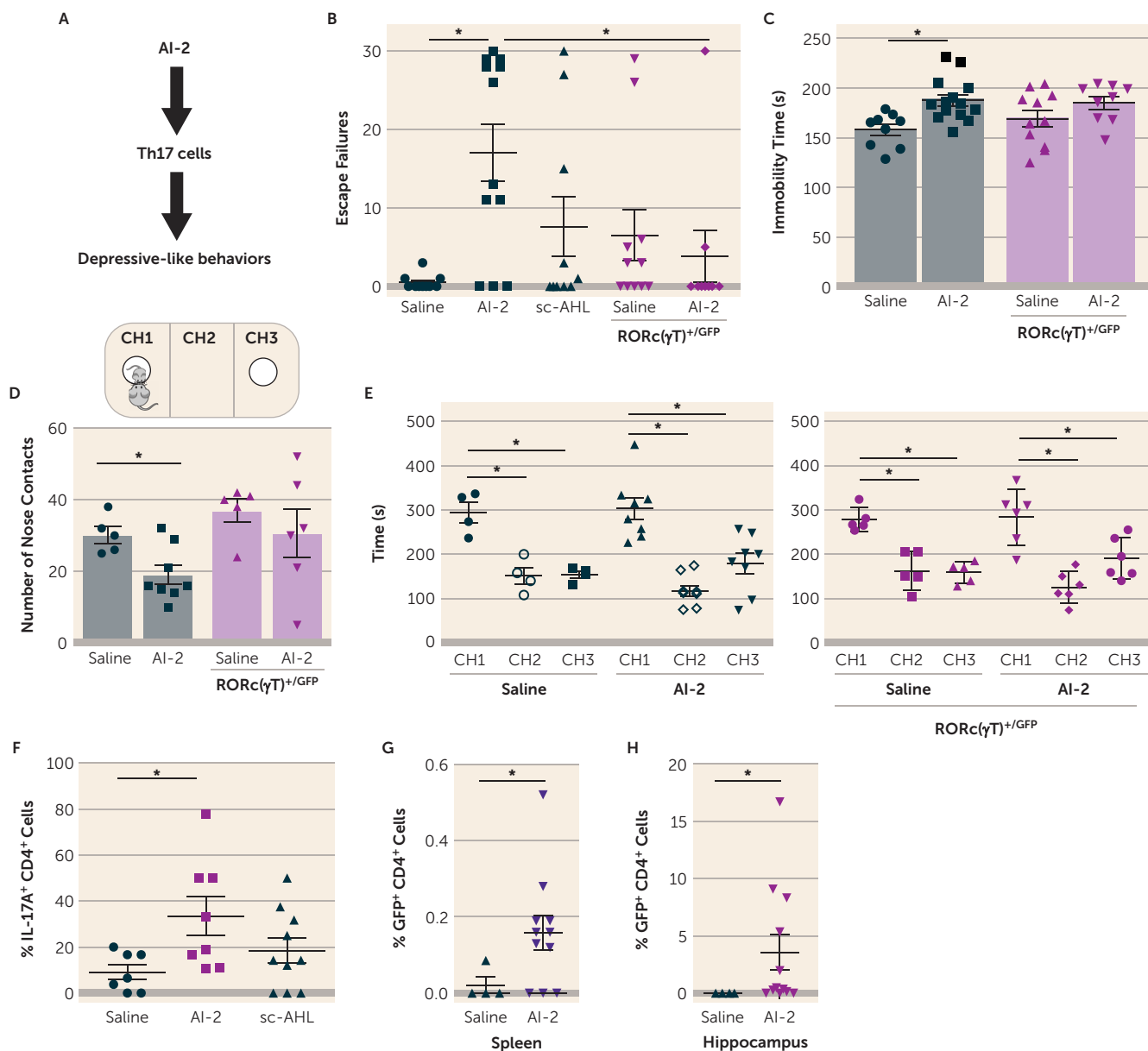
FIGURE 2. Increase in quorum-sensing molecule autoinducer-2 (AI-2) level with segmented filamentous bacteria (SFB) colonization^a

^a JAX and TAC mice were housed with or without mice from the other source for 2 weeks, or JAX mice were gavaged with SFB, and then mice were subjected to the learned helplessness paradigm. Levels of AI-2, short-chain acyl homoserine lactone (sc-AHL), and long-chain AHL (lc-AHL) (panel A–C) were analyzed by luminescence (relative light unit, RLU) in stools collected after the last foot shocks of the learned helplessness paradigm. Each symbol represents an individual mouse. Means with standard error of the mean are shown. (N=4–11 mice per group; one-way analysis of variance, $F=24.27$, $df=4, 34$, $*p<0.05$, Bonferroni post hoc test.) Levels of AI-2, sc-AHL, and lc-AHL (panels D–F) were measured in TAC mice and in germ-free (GF) mice monocolonized or not with SFB. Each symbol represents an individual mouse. Means with standard error of the mean are shown. nd=nondetectable. (N=3–4 per group; Mann-Whitney U test, $U=0$, $*p=0.0571$.) Levels of AI-2, sc-AHL, and lc-AHL (panels G–I) were measured in TAC mice subjected to learned helplessness (shocked, or S) or in non-shocked TAC mice (NS). Each symbol represents an individual mouse. Means with standard error of the mean are shown. (N=3–6 per group; Mann-Whitney U test, $U=0$, $*p<0.05$.) Panel J is a schematic diagram of the results.

(Figure 2G), whereas the levels of sc-AHL and lc-AHL remained unchanged between these two groups (Figure 2H–I), indicating that the stress of foot shocks was sufficient to increase AI-2 levels as well as to induce learned helplessness, suggesting that bacteria might adapt their behavior after the induction of stress (Figure 2J).

Since AI-2 was associated with increased susceptibility to learned helplessness in JAX mice, we tested whether AI-2 is sufficient to promote depressive-like behaviors (Figure 3A)

by daily treatments of AI-2 for 3 days before testing mice in the reduced paradigm of learned helplessness. With this paradigm, most mice do not develop learned helplessness (40, 45). AI-2 administration, but not sc-AHL, was sufficient to increase susceptibility to learned helplessness in both TAC mice (Figure 3B) and JAX mice (see Figure S1A in the online supplement). Similarly, administration of AI-2 increased immobile time in the tail suspension test (Figure 3C), often interpreted as an indication of increased despair or

FIGURE 3. T helper 17 (Th17) cell dependence of quorum-sensing molecule autoinducer-2 (AI-2)–mediated depressive-like behaviors^a

^a Panel A is a schematic diagram of the hypothesis. In panels B–F, wild-type or RORc(γT)^{+/GFP} littermate mice were injected with 5 nmol/day i.p. of AI-2, short-chain acyl homoserine lactone (sc-AHL), or saline daily for 3 days. On the third day, 1 hour after injection, mice were subjected to the reduced learned helplessness paradigm and escape failures were recorded (panel B); in another cohort of mice, immobility time was assessed in the tail suspension test (panel C); and on the fourth day, sociability was assessed with the mice used in panel C, and number of nose contacts (panel D) and time spent in each chamber (CH) (panel E) were recorded. Each symbol represents an individual mouse. Means with standard error of the mean are shown. (In panel B, N=10–12 mice per group; one-way analysis of variance (ANOVA), $F=5.955$, $df=3, 38$, $p<0.05$, Bonferroni post hoc test; in panel C, N=9–14 mice per group; one-way ANOVA, $F=4.224$, $df=3, 39$, $p<0.05$, Bonferroni post hoc test; in panel D, N=5–8 mice per group; Mann-Whitney U test, $U=5.5$, $p<0.05$; in panel E, N=4–8 mice per group; one-way ANOVA, $F=14.06$, $df=5, 25$, $p<0.05$, Bonferroni post hoc test.) In panel F, Th17 cells in the hippocampus were analyzed by flow cytometry after the learned helplessness paradigm in TAC mice. Each symbol represents an individual mouse. Means with standard error of the mean are shown. (N=7–10 mice per group; one-way ANOVA, $F=3.56$, $df=2, 24$, $p<0.05$, Bonferroni post hoc test.) In panels G and H, RORc(γT)^{+/GFP} mice were injected with 5 nmol/day i.p. of AI-2 or saline daily for 3 days, subjected to the reduced learned helplessness paradigm on the third day, and sacrificed just after the last foot shocks, and splenic (panel G) or hippocampal (panel H) GFP⁺ CD4⁺ cells were analyzed by flow cytometry. Each symbol represents an individual mouse. Means with standard error of the mean are shown. (N=4–11 mice per group; Mann-Whitney U test, $U=7.5$, $p<0.05$ [panel G], and $U=7.5$, $p=0.0586$ [panel H]).

depression. In a measure of sociability, which is frequently impaired in depression and models of depression, administration of AI-2 reduced the number of nose contacts with an unfamiliar mouse (Figure 3D), without interfering with the

preference for the CH1 chamber containing the new mouse (Figure 3E). AI-2 administration did not alter locomotor activity in a novel open field (see Figure S1C–E in the online supplement). To determine whether bacteria were required

for AI-2 prodepressive effects, we treated TAC mice and JAX mice with antibiotics to deplete the microbiota, and measured behaviors. Antibiotic treatment significantly depleted the microbiota, as shown by the reduced *Eubacterium* levels (see Figure S1F in the online supplement), and prevented AI-2 from promoting depressive-like behaviors (see Figure S1G–H in the online supplement), suggesting that AI-2 acts on bacteria rather than the host to promote depressive-like behaviors. Taken together, these findings demonstrate that AI-2 administration increased displays of multiple depressive-like behaviors that are microbiome dependent.

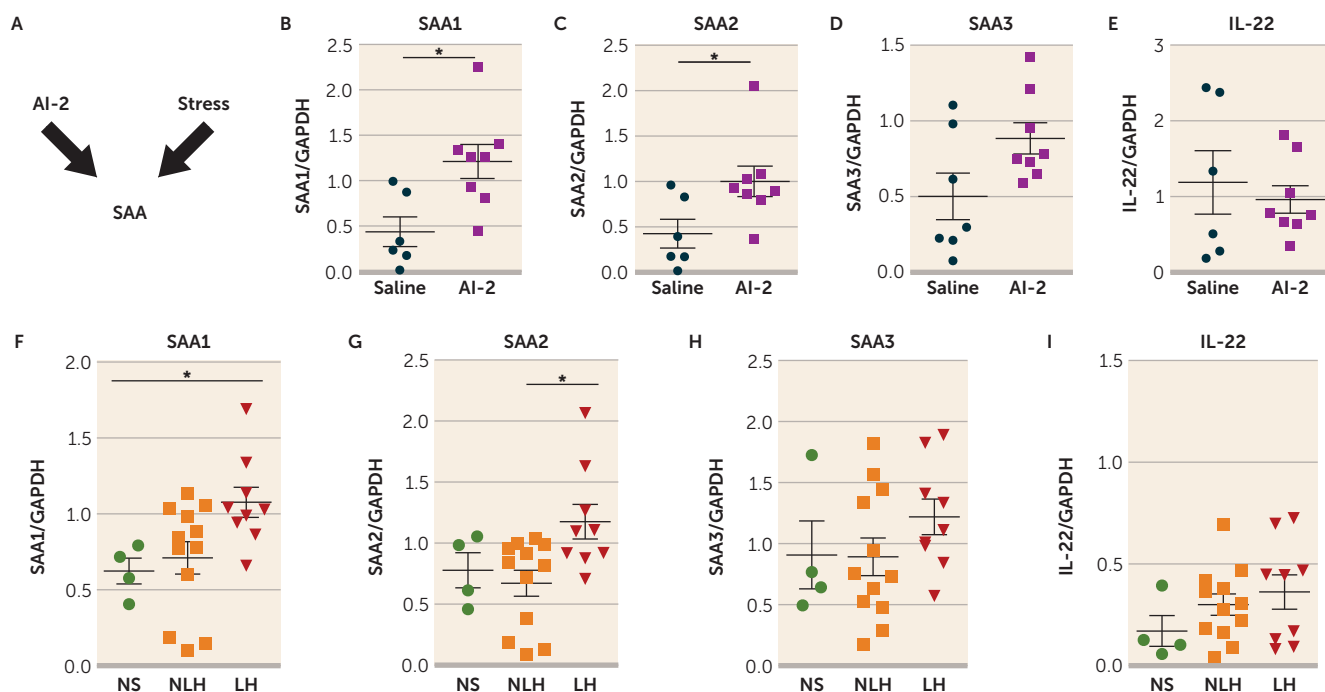
SFB is well established as promoting production of Th17 cells (34), which promote depressive-like behaviors (40, 45), and Th17 cells accumulate in the hippocampus of mice exhibiting learned helplessness (45) and are localized in the brain parenchyma (see Figure S2A in the online supplement). Introduction of SFB in JAX mice increased the accumulation of hippocampal Th17 cells after learned helplessness (see Figure S2B–D in the online supplement), whereas there was no difference in splenic Th17 cells (data not shown). We next investigated whether commensal-antigen-specific CD4⁺ cells are sufficient to promote learned helplessness in SFB⁺ Rag2^{−/−} mice. CD4⁺ cells from mice expressing a transgenic T cell receptor specific for SFB-encoded antigen (7B8) or CD4⁺ cells from littermate wild-type mice were adoptively transferred to Rag2^{−/−} mice and subjected to the reduced paradigm of learned helplessness. We found that 75% of Rag2^{−/−} mice receiving 7B8 CD4⁺ cells exhibited learned helplessness, with an average of 23 escape failures, whereas none of the Rag2^{−/−} mice receiving wild-type CD4⁺ cells exhibited learned helplessness, averaging 0.5 escape failures (see Figure S2E in the online supplement). Consistently, hippocampal Th17 cells, but not Th1 cells, were significantly increased in Rag2^{−/−} mice receiving 7B8 CD4⁺ cells and exhibiting learned helplessness, whereas receiving 7B8 CD4⁺ cells without receiving foot shocks was not sufficient to increase hippocampal Th17 cells (see Figure S2F–G). Thus, the presence of SFB in the microbiota represents one factor that modulates Th17 cell trafficking during depressive-like behaviors.

Since SFB promotes learned helplessness, promotes hippocampal Th17 cell accumulation during learned helplessness, and produces AI-2, we tested whether AI-2 administration increases Th17 cells in the hippocampus. After administration of AI-2, mice were subjected to the reduced paradigm of learned helplessness because this paradigm does not increase hippocampal Th17 cell accumulation (45), allowing for studies of factors that promote this outcome. Th17 cells were increased threefold in the hippocampus of mice receiving AI-2 compared with vehicle- or sc-AHL-treated mice (Figure 3F), whereas AI-2 had no effect in the absence of foot shocks (see Figure S2H in the online supplement) or in mice treated with antibiotics to deplete the microbiota (see Figure S2I in the online supplement), demonstrating that AI-2 promotion of Th17 cell accumulation in the hippocampus is dependent on stress (foot shocks) and the microbiota. Furthermore, even though AI-2 did not

promote Th17 cell differentiation *in vitro* (data not shown), AI-2 administration promoted Th17 cell differentiation *in vivo*, as indicated by the finding that AI-2 administration increased the percentage of GFP⁺ CD4⁺ cells both in the spleen (Figure 3G) and the hippocampus (Figure 3H) after learned helplessness in RORc(γT)^{+/GFP} mice, where a GFP reporter cDNA was knocked-in at the site of initiation of RORγt translation, leading to an important decrease in Th17 cells (40, 44, 45), indicating that AI-2 was sufficient to induce Th17 cells after shocks. Since AI-2 promotes both Th17 cell differentiation and depressive-like behaviors, we tested whether Th17 cells mediate the depression-promoting effect of AI-2 by using RORc(γT)^{+/GFP} mice. RORc(γT)^{+/GFP} mice are resistant to the induction of learned helplessness, but adoptive transfer of Th17 cells is sufficient to resensitize RORc(γT)^{+/GFP} mice to learned helplessness (41). The prodepressive effects of AI-2 administration were abolished in RORc(γT)^{+/GFP} mice (Figure 3B–D), and this was independent of SFB, AI-2, sc-AHL, lc-AHL, or SAA levels (see Figure S3 in the online supplement) or locomotor activity (see Figure S1C), which were similar in untreated wild-type and RORc(γT)^{+/GFP} mice. This indicates that Th17 cells are required to mediate AI-2-induced depressive-like behaviors.

Because Th17 cells primarily reside in the lamina propria of the small intestine in healthy mice (34), and SFB promotes Th17 cell differentiation in the small intestine via the SAA1-2/IL-22 pathway (34, 35, 55), we tested whether intestinal SAA1, SAA2, SAA3, and IL-22 levels were affected by administration of AI-2 in TAC mice after stress (Figure 4A). We found that AI-2 administration increased the intestinal expression of SAA1 and SAA2 (Figure 4B–C) but did not change the intestinal expression of SAA3 and IL-22 (Figure 4D–E) and that antibiotic treatment abolished this effect (see Figure S4A–B in the online supplement). Furthermore, mice exhibiting prolonged learned helplessness (4 weeks) also exhibited higher intestinal levels of SAA1 and SAA2 (Figure 4F–G), but not SAA3 and IL-22 (Figure 4H–I), compared with mice that did not exhibit learned helplessness or non-shocked mice. Consistent with the report of Ivanov et al. (34), SFB administration increased intestinal SAA1, SAA2, SAA3, and IL-22 levels (see Figure S4C–F). Furthermore, there were reductions of SAA1 and SAA2 levels after induction of learned helplessness in RORc(γT)^{+/GFP} mice compared with wild-type mice (see Figure S5A–D in the online supplement), suggesting that RORc(γT)^{+/GFP} mice that are resilient to learned helplessness also exhibit lower levels of SAA1 and SAA2. Furthermore, injection of recombinant SAA2 increased susceptibility to learned helplessness by 50% (see Figure S5E). Taken together, these findings suggest that the increase of intestinal SAA1 or SAA2 levels after AI-2 administration might be sufficient to increase susceptibility to learned helplessness.

Since SAA promotes intestinal cytokine production, serum cytokine and chemokine levels were measured 3 to 48 hours after AI-2 treatment to determine whether inflammation might be contributing to the induction of Th17 cells and depressive-like behaviors after AI-2 treatment. The

FIGURE 4. Elevated intestinal serum amyloid protein 1 and 2 (SAA1 and SAA2) levels in mice treated with quorum-sensing molecule autoinducer-2 (AI-2)^a

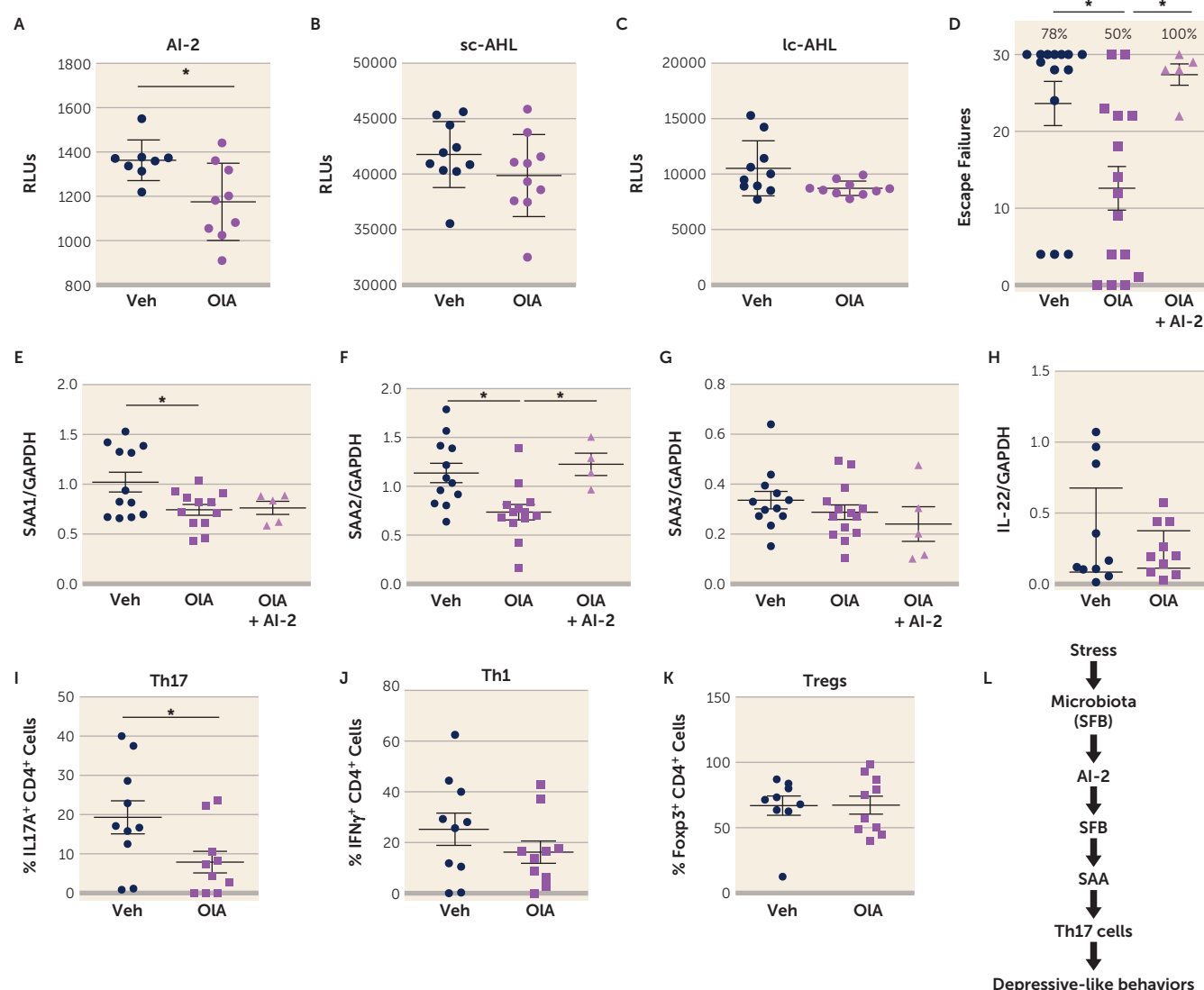
^a Panel A is a schematic diagram of the hypothesis. In panels B–E, TAC mice were injected with AI-2 (5 nmol/day i.p.) or saline daily for 3 days. Two hours after the last injections, mice were sacrificed, intestines were recovered, and RNA was extracted. Expression of SAA1, SAA2, SAA3, interleukin 22 (IL-22) (panels B–E) and GAPDH (glyceraldehyde-3-phosphate dehydrogenase) were measured by quantitative real-time polymerase chain reaction (qRT-PCR). Each symbol represents an individual mouse. Means with standard error of the mean are shown. (N=6–8 mice per group; * $p < 0.05$, Mann and Whitney U=5 (panel B), U=8 (panel C)). In panel F–I, TAC mice were not shocked (NS) or subjected to learned helplessness and were retested every week for 4 weeks and divided into two categories: those that did not develop learned helplessness or recovered during the 4 weeks of testing (NLH) and those that developed learned helplessness and remained learned helpless for 4 weeks (LH; failed to escape in >15 of the 30 trials every week). Just after the last foot shocks of the fourth week of testing, mice were sacrificed, intestines were recovered, and RNA was extracted. Expression of SAA1, SAA2, SAA3, IL-22 (panel F–I) and GAPDH were measured by qRT-PCR. Each symbol represents an individual mouse. Means with standard error of the mean are shown. (N=4–12 mice per group; one-way analysis of variance, $F=4.256$ $df=2, 24$ [panel F], $F=4.66$, $df=2, 24$ [panel G], * $p < 0.05$ Bonferroni post hoc test.)

prototypical proinflammatory cytokines known to induce depressive-like behavior—IL-1, IL-6, and TNF (36, 38)—were not affected by AI-2 treatment (see Figure S6 in the online supplement). However, there were increased serum levels of IL-2, IL-13, IL-17A, and G-CSF and decreased levels of IL-4, IL-5, IL-12, GM-CSF, CXCL1, CCL2, and CCL5 after AI-2 treatment (see Figure S6) suggesting a remodeling of the inflammatory landscape by AI-2.

A screen of natural compounds identified oleic acid as a potential AI-2 inhibitor (56). We tested whether in vivo administration of oleic acid prevented the production of AI-2 and the induction of learned helplessness. Oleic acid administration reduced fecal levels of AI-2, but not sc-AHL or lc-AHL in mice subjected to the learned helplessness paradigm (Figure 5A–C), confirming the ability of oleic acid to inhibit AI-2 production in vivo. Oleic acid reduced the susceptibility to learned helplessness of TAC mice from an average of 24 failures out of 30 trials to 13 failures, and it reduced the percentage of learned helpless mice from 78% to 40%, suggesting an antidepressant action of oleic acid (Figure 5D). The coadministration of AI-2 with oleic acid abolished this antidepressant effect, resulting in an average of 27 failures out

of 30 trials (Figure 5D), demonstrating the requirement of AI-2 in the antidepressant effect of oleic acid. As expected, levels of factors downstream of AI-2, SAA1, and SAA2, but not SAA3 or IL-22 levels, in the intestine were reduced by oleic acid administration (Figure 5E–H) after learned helplessness. However, only SAA2 levels were restored to vehicle levels after AI-2 coadministration, suggesting that SAA2 mediates AI-2-dependent depressive-like behaviors. Furthermore, the percentage of Th17 cells was also reduced in oleic acid-treated mice, whereas Th1 and regulatory T cells (Tregs) were not affected (Figure 5I–K). This reduction of Th17 cells was not associated with changes in gut permeability (see Figure S7 in the online supplement). Altogether, these data provide evidence for a new circuit involving SFB/AI-2/SAA2/Th17 cells in promoting depressive-like behaviors after stress in mice (Figure 5L).

To determine whether the findings in mice are relevant for humans, we analyzed the levels of IL-17A, SAA, AI-2, and SFB in the stools of 10 patients with a current primary diagnosis of major depressive disorder and 10 healthy matched subjects. We found that the IL-17A level was increased approximately eightfold in patients with current

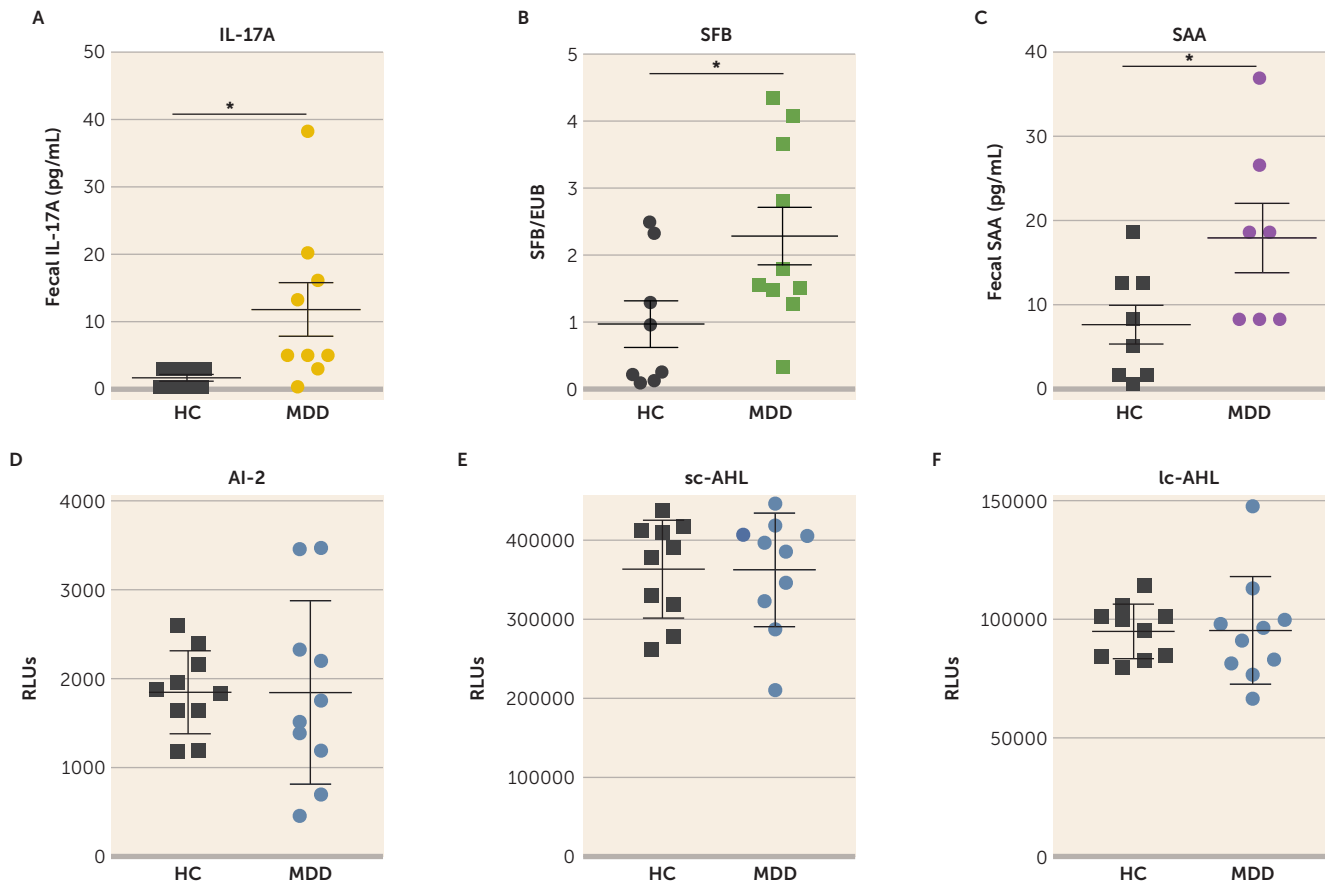
FIGURE 5. Antidepressant properties of oleic acid^a

^a TAC mice were injected with 5 nmol/day i.p. of oleic acid (OIA) or vehicle (Veh), daily for 2 weeks, and on the 3 last days of injection, some mice received 5 nmol i.p. of quorum-sensing molecule autoinducer-2 (AI-2) or vehicle daily. On the last day of treatment, mice were subjected to the learned helplessness paradigm. Levels of AI-2, short-chain acyl homoserine lactone (sc-AHL), and long-chain AHL (lc-AHL) (panels A–C) were measured in the stools immediately after the last foot shock. Each symbol represents an individual mouse. Means with standard error of the mean are shown. RLU=relative light unit. (N=8–10 per group; Mann-Whitney U test, U=13, *p<0.05.) Escape failures were recorded, and in panel D, mean and standard error of the mean are shown, and the percentage of mice exhibiting learned helplessness (failing to escape in >15 of the 30 trials) is shown above each group. Each symbol represents an individual mouse. (N=5–15 per group; one-way analysis of variance [ANOVA], F=6.054, df=2, 31, *p<0.05 Bonferroni post hoc test.) Intestinal expression of serum amyloid protein 1, 2, and 3 (SAA1, SAA2, SAA3), interleukin 22 (IL-22) (panels E–H) and GAPDH (glyceraldehyde-3-phosphate dehydrogenase) were measured by quantitative real-time polymerase chain reaction. Each symbol represents an individual mouse. Means with standard error of the mean are shown. (N=4–14; one-way ANOVA, F=3.809, df=2, 26, *p<0.05 [panel E], F=6.958, df=2, 26, *p<0.05 [panel F]). T helper 17 (Th17), Th1, and regulatory T cells (Tregs) (panels I–K) cells were analyzed in the hippocampus. Each symbol represents an individual mouse. Means with standard error of the mean are shown. (N=9–10 per group; Mann-Whitney U test, U=23, *p<0.05.) Panel L is a schematic diagram of the conclusion. SFB=segmented filamentous bacteria.

major depression compared with healthy subjects (Figure 6A), and SAA and SFB levels were increased approximately twofold (Figure 6B, C), whereas AI-2, sc-AHL, and lc-AHL levels did not differ between groups (Figure 6D–F). Furthermore, regression analyses showed that AI-2 levels were predicted by the presence of fecal SFB in patients with current major depression and healthy subjects; that is, SFB levels predicted AI-2 levels ($r=0.494$, $p=0.019$) (Table 1).

Similarly, SFB levels predicted SAA levels ($r=0.336$, $p=0.004$), SAA levels predicted IL-17A levels ($r=0.288$, $p=0.011$), and IL-17A levels predicted QIDS scores ($r=0.245$, $p=0.013$) (Table 1). No interaction of SFB with sc-AHL or lc-AHL was observed ($p=0.335$ and $p=0.217$, respectively). These data suggest that patients with current major depression have a dysregulation of the intestinal SFB/AI-2/SAA/IL-17A circuit.

FIGURE 6. Dysregulation of the SFB/AI-2/SAA/IL-17A circuit in patients with current major depressive disorder^a



^a Levels of interleukin 17A (IL-17A), segmented filamentous bacteria (SFB), serum amyloid protein (SAA) (including all human isoforms), quorum-sensing molecule autoinducer-2 (AI-2), short-chain acyl homoserine lactone (sc-AHL), and long-chain AHL (lc-AHL) (panels A–F) were analyzed in stool samples from patients with current major depression (MDD) and healthy control subjects (HC), using multiplex approach (panels A, C), quantitative real-time polymerase chain reaction (panel B), or reporter assay (panels D–F). (N=8–9; Mann-Whitney U test, U=8, *p=0.0065 [panel A]; N=7–8; unpaired t test, t=2.249, *p=0.0425 [panel B]; N=8–10; unpaired t test, t=2.461, *p=0.0286 [panel C]; N=10 [panels D–F]). EUB=eubacteria; RLU=relative light unit.

TABLE 1. Pearson regression analyses for AI-2, SFB, SAA, IL-17A, and QIDS score in patients with current major depressive disorder and healthy subjects^a

Dependent, Independent Variable	N	r	p	Adjusted r ²
AI-2, SFB	18	0.494	0.019	0.196
SFB, SAA	18	0.614	0.004	0.336
SAA, IL-17A	15	0.582	0.011	0.288
IL-17A, QIDS score	17	0.540	0.013	0.245

^a AI-2=quorum-sensing molecule autoinducer-2; IL-17A=interleukin-17A; QIDS=Quick Inventory of Depressive Symptomatology; SAA=serum amyloid protein; SFB=segmented filamentous bacteria.

DISCUSSION

We uncovered a novel mechanistic circuit linking the gut microbiome and bacterial products to the brain axis that regulates depressive-like behaviors in mice. SFB in the gut increases the bacterial QSM AI-2 and the levels of SAA1 and SAA2, and these increase the production of Th17 cells that promote depressive-like behaviors (55) (Figures 2–4).

Furthermore, administration of either SFB or AI-2 is sufficient to increase susceptibility to depressive-like behaviors of SPF mice with an intact microbiome. We also found that disrupting this signaling pathway by blocking AI-2 with oleic acid provides antidepressant properties. These findings reveal a signaling mechanism by which changes in bacterial products influence mood-relevant behavior.

As has previously been reported, microbiota composition was found to influence behaviors (2, 8, 57). We identified SFB, a spore-forming bacteria belonging to the Firmicutes phylum and closely related to the Clostridium family, as candidate bacteria that influence mood-relevant behaviors. This extends previously published reports that the Firmicutes are modulated in mice after stress exposure (9, 25, 58). Shifts in the composition of the two predominant phyla of the gut microbiome, Bacteroidetes and Firmicutes, have been associated with several CNS conditions (e.g., autism, stress, and Alzheimer’s disease) (59, 60). Although the composition of the gut microbiota has been associated with depressive disorders, the mechanisms whereby gut bacteria modulate

mood remain largely unknown (25, 61). We propose that induction of Th17 cells by SFB in the gut increases susceptibility to depressive-like behaviors. However, it is not excluded that other bacteria (such as *Akkermansia muciniphila* and *Mucispirillum schaedleri*, the latter being shown in another study [62] to be decreased after stress) are also involved in the modulation of depressive-like behaviors. *Akkermansia muciniphila* is known for its anti-inflammatory properties (63), which could also modulate the inflammation associated with depressive-like behaviors (36, 38). In addition to bacterial abundance, interactions between bacteria may be important in regulating behaviors, although further experiments are needed to test this hypothesis.

Our evidence indicates that the bacterial quorum-sensing molecule AI-2 can be an important conduit of signals from the gut to the brain. This was particularly evident from the finding that AI-2 administration was sufficient to promote depressive-like behaviors, which also demonstrated that gut bacterial metabolites have the capacity to modulate behaviors in SPF mice. In addition, increased availability of AI-2 increases the ratio of Firmicutes to Bacteroidetes, favoring the Firmicutes (64), which may create a vicious circle, amplifying depressive-like behavior. AI-2 is produced by SFB bacteria and is a key link between SFB and the production of Th17 cells, one mechanism by which SFB and AI-2 can promote susceptibility to depressive-like behaviors. However, we found that AI-2 did not act directly on the host, demonstrating that AI-2 mediates its effects through bacteria. Levels of AI-2 (Figure 2) but not SFB (data not shown) increased after foot shocks, suggesting that either foot shocks specifically affect SFB-dependent production of AI-2 or, more likely, other bacteria producing AI-2 are affected by foot shocks and are responsible for the increased production of AI-2. We also found increased SFB levels in AI-2-treated JAX mice after foot shocks, suggesting that AI-2 is able to increase the population of SFB (see Figure S1B in the online supplement), which contributes to the increased AI-2 production. However, because other bacteria also produce AI-2, this signaling circuit is not limited to SFB (65). Although AI-2 is normally produced in the lumen of the intestines, we used intraperitoneal administration, so further studies using intraluminal administration would more closely model its endogenous mode of production.

Reports have shown the presence of AI-2 and AHLs in humans, in particular in patients with inflammatory bowel disease (65, 66), who are known to have an elevated risk of comorbid depression (67). Consistent with this, we were also able to detect AI-2 in the stools of patients with current major depression. To our knowledge, quorum-sensing molecules have not previously been shown to modulate behaviors, but they are critical in regulating biofilm formation and bacterial virulence (53, 54). Therefore, the identification of AI-2 as a modulator of depressive-like behaviors represents a novel discovery that may help clarify mechanisms by which the gut microbiome influences behavior and mood.

Widely distributed and abundant in nature, oleic acid is a monounsaturated omega-9 fatty acid that was reported to

be deficient in patients with major depression (68) and increased in stress-resilient rats (69), suggesting that oleic acid helps in coping with stress. Oleic acid has also been associated with the maintenance of mental well-being (for reviews, see references 70–72) and treatment response to the antidepressant imipramine (73). Intake of oleic acid in women was associated with lower risk of severe depressed mood (74). Oleic acid is the predominant monounsaturated fatty acid in olive oil, and it has been proposed to contribute to the beneficial effect of olive oil (75). We confirmed that oleic acid is an AI-2 inhibitor (56) and that oleic acid exhibited antidepressant properties in the learned helplessness model of depression, which could be reversed by the addition of AI-2. This showed that the antidepressant effects of oleic acid were indeed AI-2 dependent.

Interest in the role of Th17 cells in depression has been increasing during the past several years (76). Th17 cells are usually thought of as being pathogenic in autoimmune diseases (76). Th17 cells are predominantly localized in the lamina propria of the small intestine in healthy mice, resulting from the activation of an IL-22-ILC3-SAA1/2 pathway induced in response to SFB, which only colonizes the ileum (55). We found that SAA1 and SAA2, but not SAA3, increase in mice exhibiting learned helplessness and in mice receiving AI-2, and decrease after oleic acid treatment, suggesting that the SAA1/2 pathway is induced after AI-2 treatment. Consistent with this, we found that SAA2 is sufficient to increase susceptibility to learned helplessness, and reintroduction of AI-2 in oleic acid-treated mice increased SAA2 but not SAA1. However, we did not find any difference in IL-22 levels after learned helplessness or AI-2 treatment, and IL-22 neutralization did not provide any antidepressant action (data not shown), suggesting that the ILC3 cells may not be involved in promoting Th17 cell production after stress. Altogether this suggests that after stress, AI-2 promotes the differentiation of Th17 cells independently of the IL-22-ILC3 pathway and that the IL-22-ILC3 pathway may be necessary only during the step of colonization by SFB to induce Th17 cells (55). Nevertheless, AI-2 promotes SAA1 and SAA2 production, leading to increased Th17 cell production (55) and increased hippocampal Th17 cell accumulation. Even though Th17 cells accumulate in the hippocampus after AI-2 treatment, it remains to be determined whether the Th17 cells produced in the intestine are indeed migrating to the brain. We found that AI-2 promotes Th17 cells in the brain, oleic acid reduces hippocampal Th17 cells, and SFB-specific T cell receptor CD4⁺ cells promote depressive-like behavior in Rag2^{-/-} mice, increasing hippocampal levels of Th17 cells, supporting the idea that intestinal Th17 cells migrate to the hippocampus. However, further experiments are required to determine the role of hippocampal Th17 cells in promoting depressive-like behaviors, the migratory mechanisms whereby Th17 cells exit the intestine after stress, and how intestinal Th17 cells infiltrate the brain. Indeed, we did not find differences in gut permeability after AI-2 or oleic acid treatments compared with controls, whereas both AI-2 and oleic acid modulate the

levels of hippocampal Th17 cells and behaviors. Therefore, it is possible that rather than changing gut permeability, and because AI-2 could not be detected in the blood (data not shown), AI-2 induces changes in Th17 cell migratory properties, such as the production of chemokine factors that attract Th17 cells outside of the gut. Consistent with this idea, we found changes in serum chemokine levels after AI-2 administration, but further experiments will be needed to answer this question. It is important to note that Th17 cells were recently shown to promote maternal immune activation-associated autistic traits by inducing IL-17A-dependent neurodevelopmental abnormalities in the offspring (77), suggesting that the cytokine IL-17A is sufficient to mediate some of the effects of Th17 cells in autism. The induction of Th17 cells was dependent on the presence of SFB in the ileum of the pregnant mothers (47), suggesting an important SFB/Th17 circuit in priming behaviors, even though the outcome behaviors may differ depending on the timing of induction and the location of Th17 cells.

Th17 cells have been shown to be induced by a high-salt diet (78) and to mediate dietary salt-induced neurovascular and cognitive impairments (79), reinforcing the idea that healthy diet, by preventing the increase of Th17 cells, enhances mental health.

Furthermore, we found that fecal IL-17A levels were increased in patients with current major depression and predicted QIDS scores, reinforcing the previously found contribution of Th17 cells to major depressive disorder (80, 81). Associated with a potential intestinal Th17 cell increase in major depression were increased fecal levels of SFB and SAA, whereas QSM levels did not change. This suggests that targeting the Th17 cell pathway may be sufficient to improve major depression. However, our study's sample size was small, and larger investigations are required.

Together, these data uncovered a novel SFB/AI-2/SAA1-2/Th17 cell pathway that promotes depressive-like behavior, and reducing AI-2 may provide therapeutic benefit.

AUTHOR AND ARTICLE INFORMATION

Department of Psychiatry and Behavioral Sciences (Medina-Rodriguez, Han, Oppenheimer, Beurel), Department of Biochemistry and Molecular Biology (Madorma, O'Connor, Deo, Daunert, Beurel), the Dr. John T. Macdonald Foundation Biomedical Nanotechnology Institute (Madorma, O'Connor, Deo, Daunert), and the University of Miami Clinical and Translational Science Institute (Daunert), Miller School of Medicine, University of Miami, Miami; Department of Psychiatry, Center for Depression Research and Clinical Care, University of Texas Southwestern Medical Center, Dallas (Mason, Trivedi); and Department of Psychiatry, Mulva Clinic for Neurosciences, University of Texas Dell Medical School in Austin (Nemeroff).

Send correspondence to Dr. Beurel (ebeurel@miami.edu).

Mr. Madorma and Dr. O'Connor contributed equally.

Supported by NIH grants MH104656 and MH110415. Drs. Deo and Daunert thank the National Institute of General Medical Sciences (grants R01GM047915 and R01GM127706) and the National Science Foundation (grants CHE-1506740 and ECC-08017788) for funding support. Dr. Daunert acknowledges support from the Lucille P. Markey Chair of the University of Miami. Dr. Trivedi acknowledges support from the Hersh

Foundation and the Betty Jo Hay Distinguished Chair in Mental Health at UT Southwestern Medical Center.

The authors thank Dr. Richard Jope for his constructive comments on the manuscript, Dr. Sue Michalek for her valuable help, and Dr. Elson for providing the SFB monocolonized feces.

Dr. Nemeroff has received grants or research support from NIH and the Stanley Medical Research Institute; he has served as a consultant for Acadia Pharmaceuticals, Bracket (Clintara), EMA Wellness, Fortress Biotech, Gerson Lehrman Group, Intra-Cellular Therapies, Janssen Research and Development, Magstim, Navitor Pharmaceuticals, Signant Health, Sumitomo Dainippon Pharma, Sunovion Pharmaceuticals, Taisho Pharmaceutical, Takeda, TC MSO, and Xhale; he is a stockholder in AbbVie, Antares, Celgene, Corcept Therapeutics, BI Gen Holdings, EMA Wellness, OPKO Health, Seattle Genetics, TC MSO, Trends in Pharma Development, and Xhale; he has served on scientific advisory boards for the Anxiety Disorders Association of America (ADAA), the American Foundation for Suicide Prevention (AFSP), Bracket (Clintara), the Brain and Behavior Research Foundation, the Laureate Institute for Brain Research, Signant Health, Skyland Trail, and Xhale and on boards of directors for the ADAA, the AFSP, Gratitude America, and Xhale Smart, Inc.; he has income sources or equity of \$10,000 or more from American Psychiatric Publishing, Bracket (Clintara), CME Outfitters, EMA Wellness, Intra-Cellular Therapies, Magstim, Signant Health, Takeda, and Xhale; and he has patents on a method and devices for transdermal delivery of lithium (US 6,375,990B1), a method of assessing antidepressant drug therapy via transport inhibition of monoamine neurotransmitters by ex vivo assay (US 7,148,027B2), and compounds, compositions, methods of synthesis, and methods of treatment (CRF receptor binding ligand) (US 8,551,996 B2). Dr. Trivedi has served as a consultant or on advisory boards for AcademyHealth, Alkermes, Akili Interactive, Allergan Pharmaceuticals, Arcadia Pharmaceuticals, ACI Clinical, Alto Neuroscience, Axsome Therapeutics, the American Society of Clinical Psychopharmacology (speaking fees and reimbursement), the American Psychiatric Association (Deputy Editor for the *American Journal of Psychiatry*), Avanir Pharmaceuticals, Boehringer Ingelheim, Janssen Pharmaceutical, Jazz Pharmaceutical, Johnson & Johnson Pharmaceutical Research and Development, Lundbeck Research USA, Medscape, Navitor, Otsuka America Pharmaceutical, Perception Neuroscience Holdings, Pharmerit International, Sage Therapeutics, and Takeda Global Research; he has received grants from the Cancer Prevention and Research Institute of Texas, NIDA, NIH, Johnson & Johnson, Janssen Research and Development, and the Patient-Centered Outcomes Research Institute; and he has received editorial compensation from Healthcare Global Village, Engage Health Media, and Oxford University Press. The other authors report no financial relationships with commercial interests.

Received September 19, 2019; revisions received January 8, February 21, and April 1, 2020; accepted April 3, 2020; published online July 31, 2020.

REFERENCES

1. Belmaker RH, Agam G: Major depressive disorder. *N Engl J Med* 2008; 358:55–68
2. Rogers GB, Keating DJ, Young RL, et al: From gut dysbiosis to altered brain function and mental illness: mechanisms and pathways. *Mol Psychiatry* 2016; 21:738–748
3. Mayer EA, Knight R, Mazmanian SK, et al: Gut microbes and the brain: paradigm shift in neuroscience. *J Neurosci* 2014; 34:15490–15496
4. Foster JA, McVey Neufeld KA: Gut-brain axis: how the microbiome influences anxiety and depression. *Trends Neurosci* 2013; 36: 305–312
5. Diaz Heijtz R, Wang S, Anuar F, et al: Normal gut microbiota modulates brain development and behavior. *Proc Natl Acad Sci USA* 2011; 108:3047–3052
6. Sudo N, Chida Y, Aiba Y, et al: Postnatal microbial colonization programs the hypothalamic-pituitary-adrenal system for stress response in mice. *J Physiol* 2004; 558:263–275

7. De Palma G, Blennerhassett P, Lu J, et al: Microbiota and host determinants of behavioural phenotype in maternally separated mice. *Nat Commun* 2015; 6:7735
8. Zheng P, Zeng B, Zhou C, et al: Gut microbiome remodeling induces depressive-like behaviors through a pathway mediated by the host's metabolism. *Mol Psychiatry* 2016; 21:786–796
9. Bailey MT, Dowd SE, Galley JD, et al: Exposure to a social stressor alters the structure of the intestinal microbiota: implications for stressor-induced immunomodulation. *Brain Behav Immun* 2011; 25: 397–407
10. De Palma G, Collins SM, Bercik P, et al: The microbiota-gut-brain axis in gastrointestinal disorders: stressed bugs, stressed brain, or both? *J Physiol* 2014; 592:2989–2997
11. Moloney RD, Desbonnet L, Clarke G, et al: The microbiome: stress, health, and disease. *Mamm Genome* 2014; 25:49–74
12. Desbonnet L, Garrett L, Clarke G, et al: Effects of the probiotic *Bifidobacterium infantis* in the maternal separation model of depression. *Neuroscience* 2010; 170:1179–1188
13. Gareau MG, Jury J, MacQueen G, et al: Probiotic treatment of rat pups normalises corticosterone release and ameliorates colonic dysfunction induced by maternal separation. *Gut* 2007; 56:1522–1528
14. O'Mahony SM, Marchesi JR, Scully P, et al: Early life stress alters behavior, immunity, and microbiota in rats: implications for irritable bowel syndrome and psychiatric illnesses. *Biol Psychiatry* 2009; 65: 263–267
15. Maslanik T, Tannura K, Mahaffey L, et al: Commensal bacteria and MAMPs are necessary for stress-induced increases in IL-1 β and IL-18 but not IL-6, IL-10, or MCP-1. *PLoS One* 2012; 7:e50636
16. García-Ródenas CL, Bergonzelli GE, Nutten S, et al: Nutritional approach to restore impaired intestinal barrier function and growth after neonatal stress in rats. *J Pediatr Gastroenterol Nutr* 2006; 43:16–24
17. Teitelbaum AA, Gareau MG, Jury J, et al: Chronic peripheral administration of corticotropin-releasing factor causes colonic barrier dysfunction similar to psychological stress. *Am J Physiol Gastrointest Liver Physiol* 2008; 295:G452–G459
18. Ait-Belgnaoui A, Durand H, Cartier C, et al: Prevention of gut leakiness by a probiotic treatment leads to attenuated HPA response to an acute psychological stress in rats. *Psychoneuroendocrinology* 2012; 37:1885–1895
19. Messaoudi M, Lalonde R, Violle N, et al: Assessment of psychotropic-like properties of a probiotic formulation (*Lactobacillus helveticus* R0052 and *Bifidobacterium longum* R0175) in rats and human subjects. *Br J Nutr* 2011; 105:755–764
20. Messaoudi M, Violle N, Bisson JF, et al: Beneficial psychological effects of a probiotic formulation (*Lactobacillus helveticus* R0052 and *Bifidobacterium longum* R0175) in healthy human volunteers. *Gut Microbes* 2011; 2:256–261
21. Huang R, Wang K, Hu J: Effect of probiotics on depression: a systematic review and meta-analysis of randomized controlled trials. *Nutrients* 2016; 8:E483
22. Ait-Belgnaoui A, Colom A, Braniste V, et al: Probiotic gut effect prevents the chronic psychological stress-induced brain activity abnormality in mice. *Neurogastroenterol Motil* 2014; 26:510–520
23. Dhakal R, Bajpai VK, Baek KH: Production of GABA (γ -aminobutyric acid) by microorganisms: a review. *Braz J Microbiol* 2012; 43: 1230–1241
24. Desbonnet L, Garrett L, Clarke G, et al: The probiotic *Bifidobacterium infantis*: an assessment of potential antidepressant properties in the rat. *J Psychiatr Res* 2008; 43:164–174
25. Jiang H, Ling Z, Zhang Y, et al: Altered fecal microbiota composition in patients with major depressive disorder. *Brain Behav Immun* 2015; 48:186–194
26. Madan A, Thompson D, Fowler JC, et al: The gut microbiota is associated with psychiatric symptom severity and treatment outcome among individuals with serious mental illness. *J Affect Disord* 2020; 264:98–106
27. Sanada K, Nakajima S, Kurokawa S, et al: Gut microbiota and major depressive disorder: a systematic review and meta-analysis. *J Affect Disord* 2020; 266:1–13
28. Stevens BR, Roesch L, Thiago P, et al: Depression phenotype identified by using single nucleotide exact amplicon sequence variants of the human gut microbiome. *Mol Psychiatry* (Epub ahead of print, January 27, 2020)
29. Valles-Colomer M, Falony G, Darzi Y, et al: The neuroactive potential of the human gut microbiota in quality of life and depression. *Nat Microbiol* 2019; 4:623–632
30. Cruz-Pereira JS, Rea K, Nolan YM, et al: Depression's unholy trinity: dysregulated stress, immunity, and the microbiome. *Annu Rev Psychol* 2020; 71:49–78
31. Macpherson AJ, Harris NL: Interactions between commensal intestinal bacteria and the immune system. *Nat Rev Immunol* 2004; 4: 478–485
32. Macpherson AJ, Uhr T: Compartmentalization of the mucosal immune responses to commensal intestinal bacteria. *Ann N Y Acad Sci* 2004; 1029:36–43
33. Ericsson AC, Hagan CE, Davis DJ, et al: Segmented filamentous bacteria: commensal microbes with potential effects on research. *Comp Med* 2014; 64:90–98
34. Ivanov II, Atarashi K, Manel N, et al: Induction of intestinal Th17 cells by segmented filamentous bacteria. *Cell* 2009; 139:485–498
35. Gaboriau-Routhiau V, Rakotobe S, Lécuyer E, et al: The key role of segmented filamentous bacteria in the coordinated maturation of gut helper T cell responses. *Immunity* 2009; 31:677–689
36. Dantzer R, O'Connor JC, Freund GG, et al: From inflammation to sickness and depression: when the immune system subjugates the brain. *Nat Rev Neurosci* 2008; 9:46–56
37. Miller AH: Depression and immunity: a role for T cells? *Brain Behav Immun* 2010; 24:1–8
38. Raison CL, Capuron L, Miller AH: Cytokines sing the blues: inflammation and the pathogenesis of depression. *Trends Immunol* 2006; 27:24–31
39. Langrish CL, Chen Y, Blumenschein WM, et al: IL-23 drives a pathogenic T cell population that induces autoimmune inflammation. *J Exp Med* 2005; 201:233–240
40. Beurel E, Harrington LE, Joep RS: Inflammatory T helper 17 cells promote depression-like behavior in mice. *Biol Psychiatry* 2013; 73: 622–630
41. Murphy AC, Lalor SJ, Lynch MA, et al: Infiltration of Th1 and Th17 cells and activation of microglia in the CNS during the course of experimental autoimmune encephalomyelitis. *Brain Behav Immun* 2010; 24:641–651
42. Ladinsky MS, Araujo LP, Zhang X, et al: Endocytosis of commensal antigens by intestinal epithelial cells regulates mucosal T cell homeostasis. *Science* 2019; 363:eaat4042
43. Bridges AA, Bassler BL: The intragenus and interspecies quorum-sensing autoinducers exert distinct control over *Vibrio cholerae* biofilm formation and dispersal. *PLoS Biol* 2019; 17:e3000429
44. Ivanov II, McKenzie BS, Zhou L, et al: The orphan nuclear receptor ROR γ directs the differentiation program of proinflammatory IL-17+ T helper cells. *Cell* 2006; 126:1121–1133
45. Beurel E, Lowell JA, Joep RS: Distinct characteristics of hippocampal pathogenic T_H17 cells in a mouse model of depression. *Brain Behav Immun* 2018; 73:180–191
46. Cheng Y, Dese S, Martinez A, et al: TNF α disrupts blood brain barrier integrity to maintain prolonged depressive-like behavior in mice. *Brain Behav Immun* 2018; 69:556–567
47. Kim S, Kim H, Yim YS, et al: Maternal gut bacteria promote neurodevelopmental abnormalities in mouse offspring. *Nature* 2017; 549:528–532
48. Love MI, Huber W, Anders S: Moderated estimation of fold change and dispersion for RNA-seq data with DESeq2. *Genome Biol* 2014; 15: 550

49. McMurdie PJ, Holmes S: Waste not, want not: why rarefying microbiome data is inadmissible. *PLOS Comput Biol* 2014; 10:e1003531
50. Reikvam DH, Erofeev A, Sandvik A, et al: Depletion of murine intestinal microbiota: effects on gut mucosa and epithelial gene expression. *PLoS One* 2011; 6:e17996
51. Wang Q, Fang CH, Hasselgren PO: Intestinal permeability is reduced and IL-10 levels are increased in septic IL-6 knockout mice. *Am J Physiol Regul Integr Comp Physiol* 2001; 281:R1013–R1023
52. Keller MB, Lavori PW, Friedman B, et al: The Longitudinal Interval Follow-Up Evaluation: a comprehensive method for assessing outcome in prospective longitudinal studies. *Arch Gen Psychiatry* 1987; 44:540–548
53. Albuquerque MT, Junqueira JC, Coelho MB, et al: Novel in vitro methodology for induction of *Enterococcus faecalis* biofilm on apical resorption areas. *Indian J Dent Res* 2014; 25:535–538
54. Rutherford ST, Bassler BL: Bacterial quorum sensing: its role in virulence and possibilities for its control. *Cold Spring Harb Perspect Med* 2012; 2:a012427
55. Sano T, Huang W, Hall JA, et al: An IL-23R/IL-22 circuit regulates epithelial serum amyloid A to promote local effector Th17 responses. *Cell* 2015; 163:381–393 (erratum in *Cell* 2016; 164:324)
56. Widmer KW, Soni KA, Hume ME, et al: Identification of poultry meat-derived fatty acids functioning as quorum sensing signal inhibitors to autoinducer-2 (AI-2). *J Food Sci* 2007; 72:M363–M368
57. Wong ML, Inserra A, Lewis MD, et al: Inflammasome signaling affects anxiety- and depressive-like behavior and gut microbiome composition. *Mol Psychiatry* 2016; 21:797–805
58. Kelly JR, Clarke G, Cryan JF, et al: Brain-gut-microbiota axis: challenges for translation in psychiatry. *Ann Epidemiol* 2016; 26:366–372
59. Finegold SM, Dowd SE, Gontcharova V, et al: Pyrosequencing study of fecal microflora of autistic and control children. *Anaerobe* 2010; 16:444–453
60. Vogt NM, Kerby RL, Dill-McFarland KA, et al: Gut microbiome alterations in Alzheimer's disease. *Sci Rep* 2017; 7:13537
61. Evrensel A, Ceylan ME: The gut-brain axis: the missing link in depression. *Clin Psychopharmacol Neurosci* 2015; 13:239–244
62. Aoki-Yoshida A, Aoki R, Moriya N, et al: Omics studies of the murine intestinal ecosystem exposed to subchronic and mild social defeat stress. *J Proteome Res* 2016; 15:3126–3138
63. Derrien M, Vaughan EE, Plugge CM, et al: *Akkermansia muciniphila* gen nov, sp nov, a human intestinal mucin-degrading bacterium. *Int J Syst Evol Microbiol* 2004; 54:1469–1476
64. Thompson JA, Oliveira RA, Djukovic A, et al: Manipulation of the quorum sensing signal AI-2 affects the antibiotic-treated gut microbiota. *Cell Rep* 2015; 10:1861–1871
65. Raut N, Pasini P, Daunert S: Deciphering bacterial universal language by detecting the quorum sensing signal, autoinducer-2, with a whole-cell sensing system. *Anal Chem* 2013; 85:9604–9609
66. Landman C, Grill JP, Mallet JM, et al: Inter-kingdom effect on epithelial cells of the N-Acyl homoserine lactone 3-oxo-C12:2, a major quorum-sensing molecule from gut microbiota. *PLoS One* 2018; 13:e0202587
67. Keefer L, Kane SV: Considering the bidirectional pathways between depression and IBD: recommendations for comprehensive IBD care. *Gastroenterol Hepatol (N Y)* 2017; 13:164–169
68. Ding X, Yang S, Li W, et al: The potential biomarker panels for identification of major depressive disorder (MDD) patients with and without early life stress (ELS) by metabonomic analysis. *PLoS One* 2014; 9:e97479
69. Li J, Zhang SX, Wang W, et al: Potential antidepressant and resilience mechanism revealed by metabolomic study on peripheral blood mononuclear cells of stress resilient rats. *Behav Brain Res* 2017; 320:12–20
70. Maes M, Galecki P, Chang YS, et al: A review on the oxidative and nitrosative stress (O&NS) pathways in major depression and their possible contribution to the (neuro)degenerative processes in that illness. *Prog Neuropsychopharmacol Biol Psychiatry* 2011; 35:676–692
71. Maes M, Smith RS: Fatty acids, cytokines, and major depression. *Biol Psychiatry* 1998; 43:313–314
72. Tiemeier H, van Tuijl HR, Hofman A, et al: Plasma fatty acid composition and depression are associated in the elderly: the Rotterdam Study. *Am J Clin Nutr* 2003; 78:40–46
73. Zhao J, Jung YH, Jang CG, et al: Metabolomic identification of biochemical changes induced by fluoxetine and imipramine in a chronic mild stress mouse model of depression. *Sci Rep* 2015; 5:8890
74. Wolfe AR, Ogbonna EM, Lim S, et al: Dietary linoleic and oleic fatty acids in relation to severe depressed mood: 10 years follow-up of a national cohort. *Prog Neuropsychopharmacol Biol Psychiatry* 2009; 33:972–977
75. Waterman E, Lockwood B: Active components and clinical applications of olive oil. *Altern Med Rev* 2007; 12:331–342
76. Beurel E, Lowell JA: Th17 cells in depression. *Brain Behav Immun* 2018; 69:28–34
77. Choi GB, Yim YS, Wong H, et al: The maternal interleukin-17a pathway in mice promotes autism-like phenotypes in offspring. *Science* 2016; 351:933–939
78. Wilck N, Matus MG, Kearney SM, et al: Salt-responsive gut commensal modulates TH17 axis and disease. *Nature* 2017; 551:585–589
79. Faraco G, Brea D, Garcia-Bonilla L, et al: Dietary salt promotes neurovascular and cognitive dysfunction through a gut-initiated TH17 response. *Nat Neurosci* 2018; 21:240–249
80. Chen Y, Jiang T, Chen P, et al: Emerging tendency towards auto-immune process in major depressive patients: a novel insight from Th17 cells. *Psychiatry Res* 2011; 188:224–230
81. Schiweck C, Valles-Colomer M, Arolt V, et al: Depression and suicidality: a link to premature T helper cell aging and increased Th17 cells. *Brain Behav Immun* 2020; 87:603–609